Supporting Information

1. Materials and methods

Materials

All reagents were obtained commercially unless otherwise noted. All solvents were dried and distilled by standard procedures. Deionized high-purity water (18.2 MΩ cm) obtained from a Purelab Option (USF Elga) water purification system. Pyrrole was dried over Na_2SO_4 and distilled under Ar.

Methods

Analytical thin-layer chromatography (TLC) was carried out using Merck silica gel 60 F-254 plates (precoated sheets, 0.2 mm thick, with fluorescence indicator F254). The spots were visualized directly or through illumination with UV lamp (λ = 254/365 nm). Column chromatography purification was carried out on silica gel (silica gel for flash chromatography, 40-63 μm, VWR).

Spectroscopic measurements

^{1}H, ^{31}P and ^{13}C NMR spectra were acquired on a Bruker Avance III 300 MHz spectrometer at room temperature (at 300 MHz, 121 MHz and 75 MHz, respectively). Chemical shifts are given in parts per million (ppm), referenced on the δ scale by using residual non-deuterated solvent signals as internal standard for ^{1}H and ^{13}C NMR spectroscopy and external phosphonic acid (H_3PO_4) for ^{31}P NMR spectroscopy. The coupling constants are expressed in units of frequency (Hz). In the carbon numbering used in the spectra description, the atoms of the phenyl residue connected to the *meso*- position of the macrocycle are labeled as first, and the protons are labeled accordingly. FT-IR spectra were registered on FT-IR Perkin Elmer Spectrum 65 spectrophotometers using ATR accessory. The UV–vis spectra were recorded using a Jasco V-550 spectrophotometer in a rectangular quartz cells (Hellma, 100-QS, 45 × 12.5 × 12.5 mm, light path 10 mm, chamber volume 3.5 mL). Fluorescence spectroscopic studies were performed using a HORIBA Jobin Yvon Fluorolog spectrophotometer (software FluorEssence) with a standard fluorometer cell (Labbox, LB Q, 10 mm). Emission spectra were recorded after excitation at the corresponding wavelength (shutter: Auto Open, excitation slit = 3 nm and emission slit = 3 nm). All fluorescence spectra were corrected.

Mass spectrometry

Accurate (HR) mass measurements were recorded on a MicrOTOFQ II (Bruker) apparatus equipped with an electrospray ionization (ESI) source. A $CHCl_3$/MeOH (1:1) solution was used for the analysis.

2. Synthesis of porphyrins M(TPPP) and M(TPPP-A)

The synthesis of free-base porphyrin H_2(TPPP) has been meticulously optimized. One synthetic approach to H_2(TPPP) is based on the introduction of the four diethoxyphosphoryl substituents on zinc *meso*-tetra(4-bromophenyl)porphyrinate (Zn(TPPBr)) using the Pd-catalyzed phosphonylation reaction.[1,2] The free base porphyrin H_2(TPPBr) can be obtained through a known procedure from commercially available 4-bromobenzaldehyde and pyrrole in 30% yield.[3] Purification of H_2(TPPBr) and Zn(TPPBr) by column chromatography is tedious due to their low solubility in all typical organic solvents, including chlorinated ones. Previous studies have also shown that replacing diethyl phosphite[2] with triisopropyl phosphite[4] in this procedure results in a significant decrease in yield from 68% to 43%.

Thus, the introduction of the diethoxyphosphoryl group in the aldehyde molecule following the classical condensation of pyrrole and diethyl (4-formylphenyl)phosphonate (**1**) under acidic conditions is more convenient, in particular when H_2(TPPP) should be prepare in gram-scale (Scheme 1). This strategy was significantly simplified by preparing 4-(diethoxyphosphoryl)benzaldehyde from commercially available 4-bromobenzaldehyde and diethyl phosphite in the presence of a Pd(0) catalyst in toluene at 80 °C.[5] Under these experimental conditions, protecting the aldehyde function[6] is no longer required. The cyclization of the aldehyde and pyrrole can be achieved using either propionic acid[6,7] (Adler-Longo reaction[8]) or boron trifluoroetherate[9] (Lindsey method[10]). It was reported that the targeted porphyrin could be obtained with a yield of 50% under Lindsey conditions[9] and with only 32% in propionic acid.[7] However, in our hands, the use of boron trifluoroetherate made it possible to obtain H_2(TPPP) in only 32–38% yield, but with fairly simple chromatographic purification of the mixtures. It is worth to note that studied condensation reaction proceeds smoothly only in chloroform ($CHCl_3$) containing traces of ethanol (about 0.75%),[11] which is a common stabilizer in commercial $CHCl_3$. When using chloroform stabilized by amylene, ethanol must be added to the reaction mixture, as the cyclization does not occur without it.

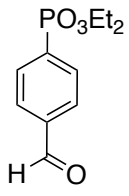

Diethyl (4-formylphenyl)phosphonate (1).[5] A dried 250 mL two-necked flask equipped with a magnetic stirrer and a back-flow condenser was charged under Ar with 4-bromobenzaldehyde (4.00 g, 21.6 mmol), $Pd(PPh_3)_4$ (100 mg, 0.87 mmol, 4 mol%) and toluene /Et_3N mixture (56 mL, 1:1 v/v)). Then diethyl *H*-phosphonate (3.3 mL, 26.00 mmol, 1.2 equiv.) was added and the mixture was stirred and heated at 80 °C for 12 h. After evaporation under reduced pressure, the residue was purified by column chromatography using a mixture CH_2Cl_2/EtOAc (1:1 v/v) as an eluent. The target compound was obtained as a yellow oil in 64% yield (3.35 g). The spectroscopic data of the obtained product were in agreement with those reported in the literature.[5]

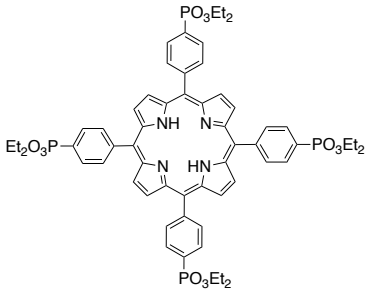

5,10,15,20-Tetrakis[(4-(diethoxyphosphoryl)phenyl]porphyrin (H_2(TPPP)).[6,9] A 1 mL two-necked flask equipped with a magnetic stirrer and a back-flow condenser was charged with compound **1** (2.03 g, 8.40 mmol) in chloroform (765 mL) stabilized with ethanol (0.75%). The reaction mixture was started for 30 min while bubbling N_2. Then freshly distilled pyrrole (583 µL, 8.40 mmol, 1 equiv.) and $BF_3{\cdot}OEt_2$ (770 µL, 6.23 mmol, 0.74 equiv.) were added and the reaction mixture was stirred at room temperature for 1 h. Then DDQ (5.72 g, 25.20 mmol, 3 equiv.) was added followed by Et_3N (1.5 mL) and the reaction mixture was stirred for 1 h. The solvent was removed under reduced pressure and the residue was purified by column chromatography on silica gel using CH_2Cl_2/CH_3OH (97:3 v/v) as an eluent. The porphyrin H_2(TPPP) was isolated as a purple solid in 35 % yield (3.41 g). The yield can probably be increased by decreasing loading of $BF_3{\cdot}OEt_2$ to 0.27 equiv..[9] ^{1}H NMR (300 MHz, $CDCl_3$, 298 K): δ_H 8.88 (s, 8 H, β-H), 8.38 (dd, $^3J_{H\text{-}H}$ = 8.0 Hz, $^4J_{H\text{-}P}$ = 4.1 Hz, 8 H, 2-H_{Ph}), 8.27 (dd, $^3J_{H\text{-}H}$ = 8.0 Hz, $^3J_{H\text{-}P}$ =13.0 Hz, 8 H, 3-H_{Ph}), 4.50–4.38 (m, 16 H, OCH_2), 1.57 (t, $^3J_{H\text{-}H}$ = 7.1 Hz, 24 H, Me) ppm. ^{31}P{^{1}H} NMR (121 MHz, $CDCl_3$, 298 K): δ_P 18.77 ppm. UV–vis (CH_2Cl_2): λ_{max} 417, 513, 550, 590, 645 nm. FT-IR (neat): υ_{max} 3316 (w), 3104 (w), 2983 (w), 2901 (w), 1602 (m), 1471 (w), 1396 (w), 1247 (s, P=O), 1048 (w), 1014 (s, P–O), 965 (s), 762 (s), 573 (s) cm^{-1}.

The spectroscopic data of the obtained product were in agreement with those reported in the literature.[6]

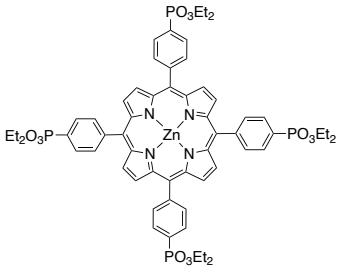

{5,10,15,20-Tetrakis[(4-(diethoxyphosphoryl)phenyl]porphyrinato}zinc(II) (Zn(TPPP)).[2] A solution of zinc acetate dihydrate (241 mg, 1.10 mmol, 20 equiv.) in methanol (12 mL) was added to a solution of porphyrin H_2(TPPP) (63 mg, 0.055 mmol) in chloroform (24 mL). The reaction mixture was stirred at room temperature for 12 h. Then, the reaction mixture was washed with water (2 × 30 mL) and the organic layer was dried over Na_2SO_4. The volatiles were removed under reduced pressure and the residue was purified by column chromatography using a mixture $CHCl_3$/MeOH (96:4 v/v) as an eluent. The Zn(TPPP) complex was obtained as a violet solid. Yield: 90% (60 mg). ^{1}H NMR (300 MHz, $CDCl_3/CD_3OD$, 2:1 v/v, 298 K): δ_H 8.80 (s, 8H; β-H), 8.32 (dd, $^3J_{H\text{-}H}$ = 8.0 Hz, $^4J_{H\text{-}P}$ = 4.1 Hz, 8H, 2-H_{Ph}), 8.32 (dd, $^3J_{H\text{-}P}$ = 12.4 Hz, $^3J_{H\text{-}H}$ = 7.5 Hz, 8H, 3-H_{Ph}), 4.43–4.27 (m, 16H, OCH_2), 1.49 (t, 24H, $^3J_{H\text{-}H}$ = 7.0 Hz, Me) ppm. ^{31}P{^{1}H} NMR ($CDCl_3/CD_3OD$, 2:1 v/v, 298 K): δ_P 18.26 ppm. UV–vis (CH_2Cl_2): λ_{max} [logε (M^{-1} cm^{-1})] 423 (5.58), 550 (4.23), 592 (sh) nm. FT-IR (neat): υ_{max} 2979 (m), 2902 (m), 1598 (m), 1523 (w), 1482 (w), 1441 (w), 1390 (m), 1337 (w), 1245 (s, P=O), 1230 (s, P=O), 1162 (w), 1129 (s), 1097 (w), 1049 (s, P–O) , 1013 (s, P–O), 993 (s, P–O), 944 (s, P–O), 990, 788

(s), 763 (s), 714 (s), 580 (s) cm^{-1}. HRMS (ESI+): *m/z* calcd. for 1/2($C_{60}H_{64}N_4Na_2O_{12}P_4Zn$) $[M+2Na]^{2+}$ 633.12791; found 633.12818; calcd. for $C_{60}H_{64}N_4NaO_{12}P_4Zn$ $[M+Na]^+$ 1243.26549 found 1243.26096. The spectroscopic data of the obtained product were in agreement with those reported in the literature.[2]

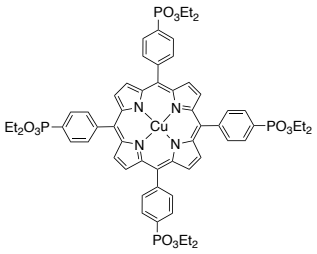

{5,10,15,20-Tetrakis[(4-(diethoxyphosphoryl)phenyl]porphyrinato}copper(II) (Cu(TPPP)).[9] A solution of copper(II) acetate monohydrate (100 mg, 0.55 mmol, 6.4 equiv.) in methanol (15 mL) was added to a solution of porphyrin H_2(TPPP) (100 mg, 0.086 mmol) in chloroform (40 mL). The reaction mixture was stirred at room temperature for 1 h. Then, the reaction mixture was washed with water (2 × 30 mL) and the organic layer was dried over Na_2SO_4. The volatiles were removed under reduced pressure and the residue was purified by column chromatography using a mixture $CHCl_3$/MeOH (94:6 v/v) as an eluent. The Cu(TPPP) complex was obtained as a red solid. Yield: 100% (105 mg). FT-IR (neat): υ_{max} 2978 (w) 2902 (w), 1599 (m), 1366, 1598 (m), 1520 (w), 1475 (w), 1441 (w), 1388 (m), 1344 (w), 1243 (s, P=O), 1206 (w), 1183 (w), 1161 (w), 1129 (s, P=O), 1098 (w), 1047 (s, P–O) , 1013 (s, P–O), 996 (s, P–O), 951 (s, P–O), 934, 790 (s), 763 (s), 716 (s), 583 (s) cm^{-1}.

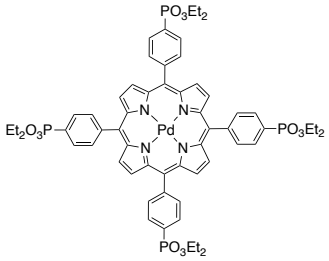

{5,10,15,20-Tetrakis[(4-(diethoxyphosphoryl)phenyl]porphyrinato}palladium(II) (Pd(TPPP)). A solution of palladium acetate (305 mg, 1.36 mmol, 7.8 equiv.) in acetonitrile (40 mL) was added to a solution of porphyrin H_2(TPPP) (200 mg, 0.173 mmol) in chloroform (40 mL). The reaction mixture was stirred at reflux for 1 h and then the volatiles were removed under reduced pressure. The residue was purified by column chromatography using a mixture CH_2Cl_2/MeOH (97:3 v/v) as an eluent. Complex Pd(TPPP) was obtained as a brown solid. Yield: 93% (204 mg). ^{1}H NMR (300 MHz, $CDCl_3$, 298 K): δ_H 8.82 (s, 8H, β-H), 8.34–8.29 (m, 8H, 2-H_{Ph}), 8.29–8.21 (m, 8H, 3-H_{Ph}), 4.49–4.35 (m, 16H, OCH_2), 1.55 (t, $^3J_{H\text{-}H}$ = 7.1 Hz, 24H, Me) ppm. $^{13}C\{^1H\}$ NMR (75 MHz, $CDCl_3$, 298 K): δ_C 145.6 (d, $^4J_{C\text{-}P}$ = 3.2 Hz, 4C, 1-C_{Ph}), 141.3 (s, 8C, α-C), 134.1 (d, $^3J_{C\text{-}P}$ = 15.1 Hz, 8C, 2-C_{Ph}), 131.3 (s, 8C, β-C), 130.1 (d, $^2J_{C\text{-}P}$ = 10.1 Hz, 8C, 3-C_{Ph}) 128.4 (d, $^1J_{C\text{-}P}$ = 188.9 Hz, 4C, 4-C_{Ph}), 120.9 (s, 4C, *meso*-C), 64.5 (d, $^2J_{C\text{-}P}$ = 5.6 Hz, 8C, OCH_2), 16.6 (d, $^3J_{C\text{-}P}$ = 7.0 Hz, 8C, Me) ppm. $^{31}P\{^1H\}$ NMR (121 MHz, $CDCl_3$, 298 K): δ_P 18.73 ppm. UV–vis (CH_2Cl_2) : λ_{max} [logε (M^{-1} cm^{-1})] 415 (5.44), 522 (4.43), 554 (3.51) nm. FT-IR (neat): υ_{max} 2981 (w), 1599 (m), 1550 (w), 1441 (w), 1389 (m), 1352 (w), 1245 (s, P=O), 1162 (w), 1129 (m), 1098 (w), 1049 (w), 1010 (s, P–O) , 949 (s, P–O), 939 (s, P–O), 793 (s), 764 (s), 712 (m), 588 (s) cm^{-1}. HRMS (ESI+): *m/z* calcd. for 1/2($C_{60}H_{66}N_4O_{14}P_4Pd$) $[M+2H]^{2+}$ 632.1336, found 632.1334; calcd. for 1/3($C_{120}H_{128}Na_3N_8O_{24}P_8Pd_2$) $[2M+3Na]^{3+}$ 864.4912, found 864.4908; calcd. for

$C_{60}H_{65}N_4O_{12}P_4Pd$ $[M+H]^+$ 1263.2599, found 1263.2580; calcd. for $1/3(C_{240}H_{254}Na_3N_{16}O_{48}P_{16}Pd_4)$ $[4M+3Na]^{3+}$ 1705.3299, found 1707.3257; calcd. for $1/2(C_{180}H_{192}Na_3N_{12}O_{36}P_{12}Pd_3)$ $[3M+2Na]^{2+}$ 1916.3687, found 1916.3664.

Doubling the reaction time led to a reduction in product yield up to 65% likely due to decomposition of the complex in the reaction mixture.

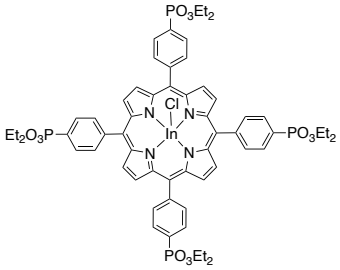

{5,10,15,20-Tetrakis[(4-(diethoxyphosphoryl)phenyl]porphyrinato}indium(III) chloride (In(TPPP)). A solution of H_2(TPPP) (100 mg, 0.087 mmol), indium(III) chloride (58 mg, 0.26 mmol, 3 equiv.) and sodium acetate (213 mg, 2.59 mmol) in glacial acetic acid (64 mL) was refluxed for 2 h. The volatiles were removed under reduced pressure and the solid residue was purified by column chromatography using a mixture CH_2Cl_2/MeOH (gradient 9:1 → 2:1 v/v) as an eluent. Complex In(TPPP) was obtained as a blue-violet solid. Yield: 70% (80 mg). ^{1}H NMR (300 MHz, $CDCl_3$, 298 K): δ_H 9.08 (s, 8H, β-H), 8.52 (br dd, $^3J_{H\text{-}H}$ = 8.0 Hz, $^4J_{H\text{-}P}$ = 4.1 Hz, 4H, 2-H_{Ph}), 8.35–8.22 (m, 12H, 2-H_{Ph} and 3-H_{Ph}), 4.50–4.35 (m, 16H, OCH_2), 1.56 (t, $^3J_{H\text{-}H}$ = 7.1 Hz, 24 H, Me) ppm.^{13}C{^{1}H} NMR (75 MHz, $CDCl_3$, 298 K): 149.2 (s, 8C, α-C), 145.5 (d, $^4J_{C\text{-}P}$ = 3.2 Hz, 4C, 1-C_{Ph}), 135.0 (d, $^3J_{C\text{-}P}$ = 14.8 Hz, 4C, 2-C_{Ph}), 134.2 (d, $^3J_{C\text{-}P}$ = 15.3 Hz, 4C, 2-C_{Ph}), 133.0 (s, 8C, β-C), 130.2 (d, $^2J_{C\text{-}P}$ = 12.7 Hz, 8C, 3-C_{Ph}), 128.6 (d, $^1J_{C\text{-}P}$ = 189.2 Hz, 4C, 4-C_{Ph}), 120.9 (s, 4C, *meso*-C), 62.7 (d, $^2J_{C\text{-}P}$ = 5.7 Hz, 8C, OCH_2), 16.6 (d, $^3J_{C\text{-}P}$ = 6.3 Hz, 8C, Me) ppm. ^{31}P{^{1}H} NMR (121 MHz, $CDCl_3$, 298 K): δ_P 18.51 ppm. UV–vis (CH_2Cl_2) : λ_{max} [logε (M^{-1} cm^{-1})] 404 (4.60), 426 (5.79), 518 (3.49), 559 (4.33), 598 (3.91) nm. FT-IR (neat): υ_{max} 3109 (w), 2978 (w), 2903 (w), 1599 (m), 1474 (w), 1392 (w), 1245 (s, P=O), 1130 (m), 1050 (s, P–O), 1008 (s) , 974 (s, P–O), 764 (m), 583 (m) cm^{-1}. HRMS(ESI+): *m/z* calcd. for $1/2(C_{60}H_{65}N_4O_{14}P_4In)$ $[M–Cl+H]^{2+}$ 636.1289, found 636.1303; $1/3(C_{120}H_{129}N_8O_{24}P_8In_2)$ $[2M–2Cl+H]^{3+}$ 847.8362, found 847.8389; $C_{60}H_{64}N_4O_{12}P_4In$ $[M–Cl]^+$ 1271.2505, found 1271.2532; $C_{60}ClH_{65}N_4O_{12}P_4In$ $[M+H]^+$ 1307.2271, found 1307.2295.

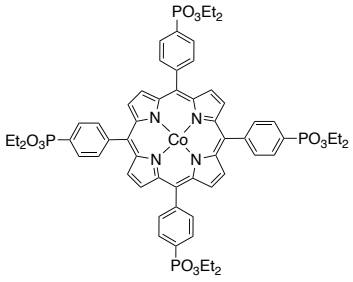

{5,10,15,20-Tetrakis[(4-(diethoxyphosphoryl)phenyl]porphyrinato}cobalt(II) (Co(TPPP)). A solution of cobalt(II) acetate tetrahydrate (92 mg, 0.52 mmol, 5.9 equiv.) in methanol (3 mL) was added to a solution of porphyrin H_2(TPPP) (103 mg, 0.089 mmol) in chloroform (13 mL). The reaction mixture was refluxed for 2 h under Ar. Then, the volatiles were removed under reduced pressure and the residue was purified by column chromatography using a mixture CH_2Cl_2/MeOH (97 : 3 v/v) as an eluent. The Co(TPPP) complex was obtained as a burgundy solid. Yield: 60% (65 mg). UV–vis (CH_2Cl_2): λ_{max} [logε (M^{-1} cm^{-1})] 412 (5.40), 438 (4.44), 528 (4.21) nm. FT-IR (neat): υ_{max} 2980 (w), 2902 (w), 1599 (m), 1444 (w), 1389 (w), 1244 (s, P=O), 1129 (m), 1046 (s, P–O), 1013 (s, P–O), 997 (w), 768

(s) cm^{-1}. HRMS(ESI+): *m/z* calcd. for $C_{60}H_{64}N_4Na_2O_{12}P_4Co$ $[M+2Na]^{2+}$ 630.6294, found 630.6306 ; calcd. for $1/3(C_{120}H_{128}Na_3N_8O_{24}P_8Co_2)$ $[2M+3Na]^{3+}$ 833.5105, found 833.5130; calcd. for $C_{60}H_{65}N_4O_{12}P_4Co$ $[M+H]^+$ 1216.2876, found 1216.2869 ; calcd. for $1/3(C_{240}H_{254}Na_3N_{16}O_{48}P_{16}Co_4)$ $[4M+3Na]^{3+}$ 1643.3630, found 1643.3672 ; calcd. for $1/2(C_{180}H_{192}Na_3N_{12}O_{36}P_{12}Co_3)$ $[3M+2Na]^{2+}$ 1845.9097, found 1845.9119.

*Synthesis of porphyrins **M(TPPP-A)**.General Procedure*. A Schlenk tube was charged with the porphyrin M(TPPP) (0.05 mmol), and the evacuation/inert gas refill cycle was repeated three times. Anhydrous CH_2Cl_2 (5 mL) and bromotrimethylsilane (25–35 equiv.) were added by syringe, and the reaction mixture was stirred for 48 h at room temperature. The volatiles were distilled under reduced pressure and MeOH (2 mL) was added, and the solution was stirred for 1 h at room temperature. Evaporation of the volatiles afforded M(TPPP-A) as a crystalline powder in quantitative yield. A low solubility of the reaction products in organic solvents has prevented their purification by column chromatography.

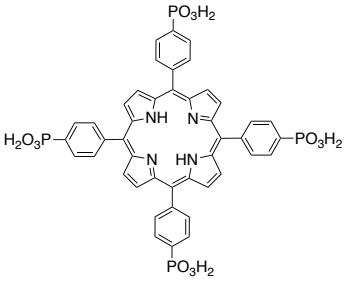

5,10,15,20-Tetrakis[(4-(dihydroxyphosphoryl)phenyl]porphyrin (H_2(TPPP-A))[1] was prepared from H_2(TPPP) (100 mg, 0.086 mmol) and bromotrimethylsilane (285 µL, 2.16 mmol, 25 equiv.). ^{1}H NMR (300 MHz, DMSO-d_6): δ_H 8.84 (s, 8H, β-H), 8.33 (dd, $^3J_{H\text{-}H}$ = 7.9 Hz, $^4J_{H\text{-}P}$ = 3.3 Hz, 8H, 2-H_{Ph}), 8.14 (dd, $^3J_{H\text{-}H}$ = 7.9 Hz, $^3J_{H\text{-}P}$ = 12.7 Hz, 8H, 3-H_{Ph}), –2.98 (br s, 2H, NH) ppm. The protons of the phosphonic acid groups were not observed due to overlapping with peaks from residual water. ^{31}P{^{1}H} NMR (121 MHz, DMSO-d_6): δ_P 12.7 (s) ppm. UV–vis (MeCN/H_2O (1:1 v/v) + 1 drop of 0.1 M NaOH): λ_{max} [logε (M^{-1} cm^{-1})] 399 (4.82), 416 (5.54), 482 (3.43), 516 (4.11), 552 (3.88), 589 (3.62), 644 (3.62) nm. FT-IR (neat): υ_{max} 3025 (w), 2890 (w), 2757 (w), 1599 (w), 1551 (w), 1486 (s), 1396 (m), 1229 (w), 1196 (w), 997 (w), 981 (w), 910 (m), 852 (m), 700 (m) cm^{-1}. The spectroscopic data of the obtained product were in agreement with those reported in the literature.[4]

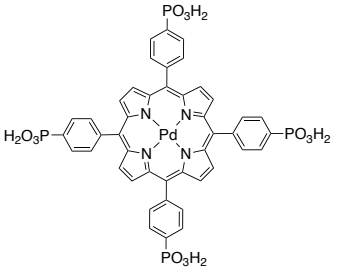

{5,10,15,20-Tetrakis[(4-(dihydroxyphosphoryl)phenyl]porphyrinato}palladium(II) (Pd(TPPP-A)) was prepared from Pd(TPPP) (80 mg, 0.063 mmol) and bromotrimethylsilane (270 µL, 2.05 mmol, 33 equiv). ^{1}H NMR (300 MHz, D_2O + 1 drop of NaOD (40% in D_2O)) : δ_H 8.77 (br s, 8H, H-β), 8.08 (br s, 16H, 2-H_{Ph} and 3-H_{Ph}) ppm.^{1}H NMR (300 MHz, DMSO-d_6): δ_H 8.78 (s, 8H, β-H), 8.27 (dd, $^3J_{H\text{-}H}$ = 7.8 Hz, $^4J_{H\text{-}P}$ = 2.0 Hz, 8H, 2-H_{Ph}), 8.12 (dd, $^3J_{H\text{-}H}$ = 7.8 Hz, $^3J_{H\text{-}P}$ = 12.7 Hz, 8H, 3-H_{Ph}) ppm.^{13}C{^{1}H} NMR (75 MHz, D_2O + 1 drop of NaOD (40% in D_2O)): δ_C 143.53 (d, $^4J_{C\text{-}P}$ = 2.3 Hz, 4C, 1-C_{Ph}), 143.43 (s, 8C, α-C), 142.80 (d, $^1J_{C\text{-}P}$ = 165.9 Hz, 4C, C-4(Ph), 136.1 (d, $^3J_{C\text{-}P}$ = 12.8 Hz, 8C, 2-C_{Ph}), 133.9 (s, 8C, C-β), 131.2 (d, $^2J_{C\text{-}P}$ = 9.0 Hz, 8C, 3-C_{Ph}), 124.1 (s, 4C, *meso*-C) ppm. ^{31}P{^{1}H} NMR (121 MHz, D_2O + 1 drop of NaOD (40% in D_2O)): δ_P 11.41 ppm. ^{31}P{^{1}H} NMR (121 MHz, DMSO-d_6): δ_P 12.3 (s) ppm.

$^{13}C\{^1H\}$ NMR (75 MHz, D_2O + 1 drop of NaOD (40% in D_2O)): δ_C 143.5 (d, $^4J_{C\text{-}P}$ = 2.2 Hz, 4C, 1-C_{Ph}), 141.1 (s, 8C, α-C), 135.3 (s, 8C, 4-C_{Ph}), 134.1 (d, $^3J_{C\text{-}P}$ = 10.8 Hz, 8 C, 2-C_{Ph},) 133.5 (s, 4C, 4-C_{Ph}), 131.8 (s, 8C, *β–C)*, 129.7 (d, $^2J_{C\text{-}P}$ = 7.5 Hz, 8C, 3-C_{Ph}), 121.7 (s, 4C*, meso*-C) ppm. UV–vis (MeCN/H_2O (1:1 v/v) + 1 drop of 0.1 M NaOH): λ_{max} [logε (M^{-1} cm^{-1})] 415 (5.33), 463 (3.78), 523 (4.23), 556 (3.29) nm. FT-IR (neat): υ_{max} 3211 (s), 1627 (m), 1454 (w), 1351 (w) , 1128 (w), 1050 (m), 1013 (w), 961 (m), 885 (w), 791 (w), 706 (w) cm^{-1}. HRMS(ESI+): *m/z* calcd. for $C_{44}H_{29}N_4O_{12}P_4Pd$ $[M–3H]^{3–}$ 344.9933, found 344.9945; calcd. for $C_{44}H_{29}N_4O_{12}P_4Pd$ $[M–2H]^{2–}$ 517.9936, found 517.9951.

Hydrolysis of diethoxyphosphoryl groups of H_2(TPPP) in concentrated hydrochloric acid (HCl) proceeded very slowly even under reflux probably due to a low solubility of starting and partially hydrolyzed porphyrins.

3. X-ray crystallography of Pd(TPPP-A)

Structure Quality Indicators

Reflections:	d min (Mo) 2Θ=50.0° 0.84	I/σ(I) 29.4	Rint 8.78%	Full 50.0° 99.9
Refinement:	Shift -0.001	Max Peak 0.9	Min Peak -0.7	GooF 1.123

Data were measured using ϕ and ω scans with Mo $K_{\alpha 1}$ radiation. The diffraction pattern was indexed and the total number of runs, and images was based on the strategy calculation from the program APEX4. The maximum resolution that was achieved was $\Theta = 25.000^{\circ}$ (0.84 Å). The unit cell was refined using SAINT V8.40B[12] on 9795 reflections, 6% of the observed reflections. Data reduction, scaling and absorption corrections were performed using SAINT V8.40B.[12] The final completeness is 99.90 % out to 25° in Θ. SADABS-2016/2[12] was used for absorption correction. wR_2(int) was 0.0780 before and 0.0675 after correction. The ratio of minimum to maximum transmission is 0.8378. The absorption coefficient μ of this material is 0.474 mm^{-1} at this wavelength ($\lambda = 0.71073$Å) and the minimum and maximum transmissions are 0.671 and 0.801. The structure was solved, and the space group *P*-1 (# 2) determined by the ShelXT[13,14] structure solution program using dual methods and refined by full matrix least squares minimisation on F^2 using version 2018/3 of ShelXL.[13,14] All non-hydrogen atoms were refined anisotropically, excepted minor disordered part of phenyl group. Hydrogen atom positions were calculated geometrically and refined using the riding model. There is a single molecule in the asymmetric unit, which is represented by the reported sum formula. In other words: *Z* is 2 and *Z'* is 1.

The crystal structure of $(Me_2NH_2)_2$[Pd(TPPP-A)$_{-2H}$] contains one solvent accessible void in the unit cell. Despite numerous attempts, no sensible solvent model could be established, and the solvent is assumed to be chaotically disordered within the voids. The crystals had been obtained from a mixture of DMF and water. The method implemented in Olex2 is based on that described by van der Sluis and Spek,[15] upon which the SQUEEZE routine in PLATON[16] is also based. The program allows to mathematically subtract the contribution of disordered solvent contained in voids within the crystal lattice from the diffraction intensities. This procedure was applied to the data file and the submitted model is based on the "solvent removed" data. Squeeze located one void (Table S6) with a volume of 777 Å^3, each of which large enough to accommodate approximately 8 molecules of DMF. From each void, the program removed the contribution of 318 electrons, corresponding to 99% of the electrons of eight DMF (40 electrons) molecules.

Table S1. Crystal Data and Structure Refinement for $(Me_2NH_2)_2[Pd(TPPP\text{-}A)_{-2H}]$.

Formula	$C_{48}H_{45}N_6O_{12}P_4Pd$
CCDC	2290735
$D_{calc.}$/ g cm^{-3}	1.254
μ/mm^{-1}	0.474
Formula Weight	1128.18
Colour	clear dark violet
Shape	needle-shaped
Size/mm^3	0.43x0.18x0.13
T/K	110.0(1)
Crystal System	triclinic
Space Group	P-1
a/Å	13.0368(4)
b/Å	13.9158(5)
c/Å	18.0430(6)
α/°	69.419(2)
β/°	81.680(2)
γ/°	78.062(2)
V/Å^3	2988.85(18)
Z	2
Z'	1
Wavelength/Å	0.71073
Radiation type	Mo $K_{\alpha 1}$
Θ_{min}/°	1.209
Θ_{max}/°	25.000
Measured Refl's.	175832
Indep't Refl's	10535
Refl's I≥2 σ(I)	8528
R_{int}	0.0878
Parameters	666
Restraints	0
Largest Peak	0.940
Deepest Hole	-0.742
GooF	1.123
wR_2 (all data)	0.1521
wR_2	0.1437
R_1 (all data)	0.0767
R_1	0.0606

A B

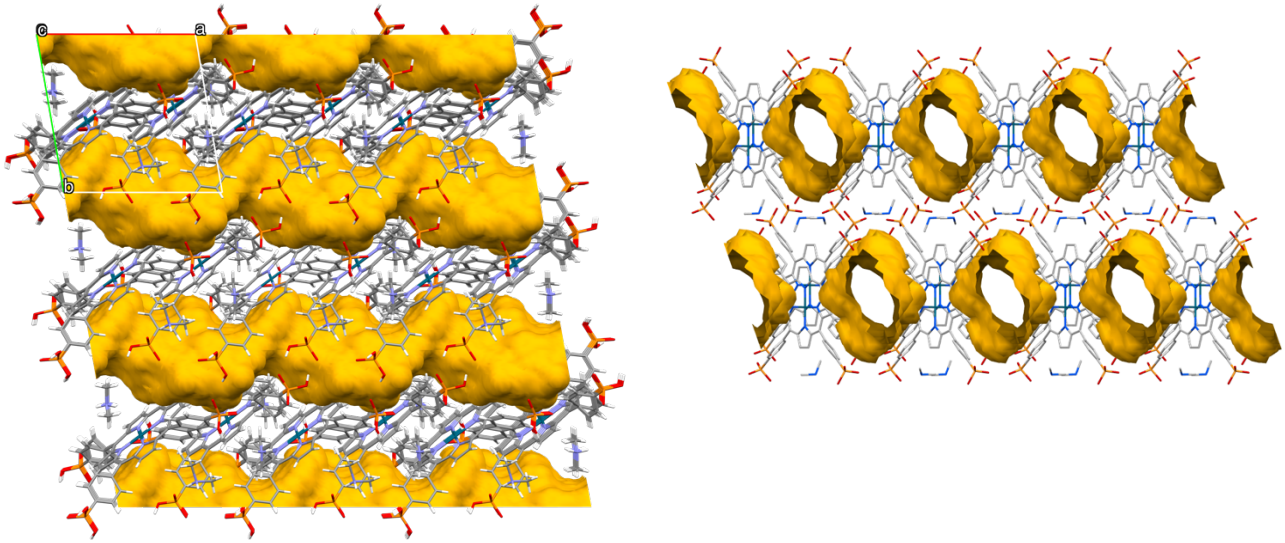

Figure S1. The structure of microporous HOF of $(Me_2NH_2)_2[Pd(TPPP\text{-}A)_{\text{-}2H}]$ showing organization of 1D pores (view along [100] (A) and [101] (B) crystallographic directions).

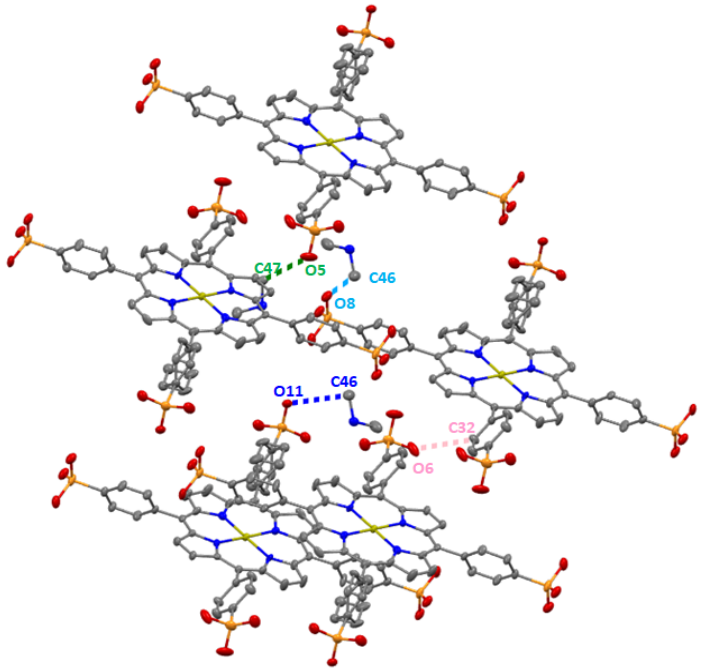

Figure S2. Schematic presentation of C–H…O bonding in the crystal $(Me_2NH_2)_2[Pd(TPPP\text{-}A)_{\text{-}2H}]$.

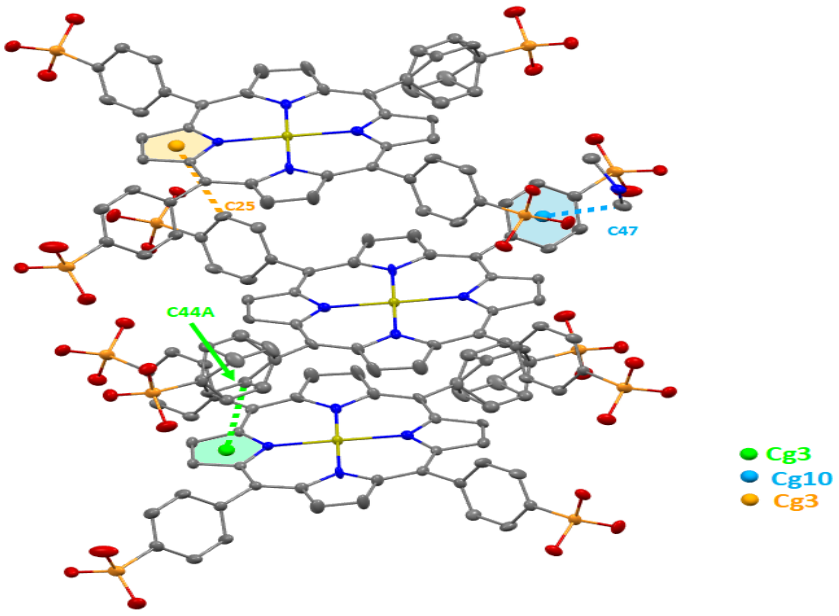

Figure S3. Schematic presentation of C—H…Cg bonding in the crystal $(Me_2NH_2)_2[Pd(TPPP\text{-}A)_{\text{-}2H}]$.

Table S2. Bond Lengths in Å for $(Me_2NH_2)_2[Pd(TPPP\text{-}A)_{\text{-}2H}]$.

Atom	Atom	Length
Pd1	N3	2.018(4)
Pd1	N1	2.021(4)
Pd1	N4	2.022(5)
Pd1	N2	2.032(4)
P1	O3	1.562(4)
P1	O2	1.506(4)
P1	O1	1.519(4)
P1	C24	1.797(5)
P4	O10	1.512(4)
P4	O12	1.566(4)
P4	O11	1.500(4)
P4	C42	1.803(5)
P3	O9	1.509(4)
P3	O8	1.529(4)
P3	O7	1.555(5)
P3	C36	1.803(5)
P2	O4	1.500(4)
P2	O6	1.549(5)
P2	O5	1.518(5)
P2	C30	1.802(5)
N3	C11	1.373(6)
N3	C14	1.376(6)
N1	C4	1.373(6)
N1	C1	1.376(7)
N4	C19	1.373(7)
N4	C16	1.380(7)
N2	C6	1.366(7)
N2	C9	1.380(7)
C21	C5	1.494(7)
C21	C26	1.390(8)
C21	C22	1.382(8)
C4	C5	1.401(7)
C4	C3	1.428(7)
C5	C6	1.379(8)
C1	C20	1.394(7)

Atom	Atom	Length
C1	C2	1.429(8)
C36	C37	1.379(8)
C36	C35	1.382(8)
C11	C10	1.402(7)
C11	C12	1.426(7)
C20	C19	1.383(8)
C20	C39	1.497(7)
C27	C10	1.483(7)
C27	C32	1.384(8)
C27	C28	1.391(8)
C37	C38	1.382(8)
C19	C18	1.425(8)
C33	C15	1.497(7)
C33	C38	1.378(8)
C33	C34	1.397(8)
C10	C9	1.394(7)
C15	C14	1.401(7)
C15	C16	1.398(7)
C2	C3	1.347(8)
C26	C25	1.401(8)
C42	C43A	1.373(10)
C42	C41A	1.395(10)
C42	C43	1.30(2)
C42	C41	1.43(2)
C12	C13	1.346(7)
C7	C8	1.341(8)
C7	C6	1.444(8)
C32	C31	1.357(8)
C28	C29	1.392(8)
C23	C22	1.384(8)
C23	C24	1.366(8)
C34	C35	1.385(8)
C14	C13	1.433(7)
C31	C30	1.386(8)
C29	C30	1.395(8)
C8	C9	1.436(8)

Atom	Atom	Length
C25	C24	1.397(8)
C17	C18	1.343(8)
C17	C16	1.436(8)
C43A	C44A	1.411(11)
C44A	C39	1.386(10)
C40A	C41A	1.388(12)
C40A	C39	1.388(10)
C39	C40	1.52(3)
C39	C44	1.26(3)
N5	C46	1.471(8)
N5	C45	1.478(8)
N6	C47	1.458(7)
N6	C48	1.499(7)
C40	C41	1.37(3)
C44	C43	1.42(3)

Table S3. Bond Angles in ° for $(Me_2NH_2)_2[Pd(TPPP\text{-}A)_{-2H}]$.

Atom	Atom	Atom	Angle
N3	Pd1	N1	178.98(18)
N3	Pd1	N4	90.25(17)
N3	Pd1	N2	89.94(16)
N1	Pd1	N4	90.03(17)
N1	Pd1	N2	89.78(16)
N4	Pd1	N2	179.45(19)
O3	P1	C24	104.2(2)
O2	P1	O3	111.4(2)
O2	P1	O1	113.3(2)
O2	P1	C24	108.3(2)
O1	P1	O3	110.6(3)
O1	P1	C24	108.6(2)
O10	P4	O12	109.7(3)
O10	P4	C42	108.1(2)
O12	P4	C42	104.3(3)
O11	P4	O10	113.7(2)
O11	P4	O12	112.3(2)
O11	P4	C42	108.2(3)
O9	P3	O8	115.4(2)
O9	P3	O7	111.1(3)
O9	P3	C36	109.6(2)
O8	P3	O7	109.0(3)
O8	P3	C36	107.6(3)
O7	P3	C36	103.4(2)
O4	P2	O6	111.8(3)
O4	P2	O5	118.4(3)
O4	P2	C30	110.2(3)
O6	P2	C30	106.2(3)
O5	P2	O6	104.8(3)
O5	P2	C30	104.6(3)
C11	N3	Pd1	127.4(3)
C11	N3	C14	106.0(4)
C14	N3	Pd1	126.6(3)
C4	N1	Pd1	126.6(3)
C4	N1	C1	106.9(4)
C1	N1	Pd1	126.1(3)
C19	N4	Pd1	126.5(4)
C19	N4	C16	106.3(4)
C16	N4	Pd1	127.1(3)
C6	N2	Pd1	126.0(3)
C6	N2	C9	107.3(4)
C9	N2	Pd1	126.3(3)
C26	C21	C5	121.2(5)
C22	C21	C5	120.0(5)
C22	C21	C26	118.8(5)
N1	C4	C5	126.1(5)
N1	C4	C3	109.5(5)
C5	C4	C3	124.4(5)
C4	C5	C21	117.1(5)
C6	C5	C21	119.2(5)
C6	C5	C4	123.7(5)
N1	C1	C20	126.2(5)
N1	C1	C2	108.5(5)
C20	C1	C2	125.2(5)
C37	C36	P3	119.4(4)
C37	C36	C35	118.4(5)
C35	C36	P3	122.3(4)
N3	C11	C10	125.7(5)
N3	C11	C12	109.6(4)
C10	C11	C12	124.7(5)
C1	C20	C39	116.7(5)
C19	C20	C1	124.2(5)
C19	C20	C39	119.0(5)
C32	C27	C10	122.5(5)
C32	C27	C28	117.3(5)
C28	C27	C10	120.2(5)
C36	C37	C38	121.3(5)
N4	C19	C20	126.3(5)
N4	C19	C18	109.4(5)
C20	C19	C18	124.2(5)
C38	C33	C15	120.4(5)
C38	C33	C34	118.9(5)
C34	C33	C15	120.8(5)
C11	C10	C27	118.0(4)
C9	C10	C11	124.2(5)
C9	C10	C27	117.8(5)
C14	C15	C33	118.1(5)
C16	C15	C33	117.1(5)
C16	C15	C14	124.8(5)
C33	C38	C37	120.4(5)
C3	C2	C1	108.2(5)
C21	C26	C25	120.7(5)
C43A	C42	P4	122.1(5)
C43A	C42	C41A	118.0(6)
C41A	C42	P4	119.8(5)
C43	C42	P4	125.3(11)
C43	C42	C41	120.3(15)
C41	C42	P4	113.6(10)
C13	C12	C11	107.9(5)
C8	C7	C6	107.5(5)
C31	C32	C27	121.4(5)
C27	C28	C29	121.4(5)
C24	C23	C22	121.7(5)
C35	C34	C33	120.0(5)
C21	C22	C23	120.3(5)
N3	C14	C15	126.0(5)

Atom	Atom	Atom	Angle
N3	C14	C13	109.8(4)
C15	C14	C13	124.1(5)
C32	C31	C30	122.4(6)
C28	C29	C30	120.4(5)
C7	C8	C9	107.8(5)
C24	C25	C26	119.5(5)
C18	C17	C16	107.0(5)
C17	C18	C19	108.1(5)
C42	C43A	C44A	121.4(7)
C39	C44A	C43A	119.2(7)
C39	C40A	C41A	120.2(7)
C40A	C41A	C42	120.9(7)
C2	C3	C4	106.9(5)
N4	C16	C15	125.1(5)
N4	C16	C17	109.3(5)
C15	C16	C17	125.4(5)
C36	C35	C34	121.1(5)
C31	C30	P2	121.3(4)
C31	C30	C29	117.1(5)
C29	C30	P2	121.6(4)
N2	C6	C5	127.1(5)

Atom	Atom	Atom	Angle
N2	C6	C7	108.8(5)
C5	C6	C7	123.9(5)
C20	C39	C40	115.7(11)
C44A	C39	C20	122.3(5)
C44A	C39	C40A	119.4(6)
C40A	C39	C20	118.3(6)
C44	C39	C20	128.2(13)
C44	C39	C40	114.6(16)
C12	C13	C14	106.7(5)
C23	C24	P1	120.7(4)
C23	C24	C25	119.0(5)
C25	C24	P1	120.2(4)
N2	C9	C10	126.4(5)
N2	C9	C8	108.6(5)
C10	C9	C8	125.0(5)
C46	N5	C45	112.5(5)
C47	N6	C48	113.2(5)
C41	C40	C39	120(2)
C39	C44	C43	125(2)
C42	C43	C44	120(2)
C40	C41	C42	117(2)

Table S4. Hydrogen Bond information for $(Me_2NH_2)_2$[Pd(TPPP-A)$_{-2H}$].

D	H	A	d(D-H)/Å	d(H-A)/Å	d(D-A)/Å	D-H-A/deg
O3	H3	O11[1]	0.84	1.67	2.500(5)	169.6
O8	H8	O5[2]	0.84	1.78	2.450(6)	135.8
O7	H7	O1[3]	0.84	1.70	2.513(5)	161.5
O6	H6	O10[4]	0.84	1.78	2.540(6)	149.8
O12	H12	O2[2]	0.84	1.77	2.534(6)	151.0
N5	H5A	O4[5]	0.91	1.79	2.700(6)	173.7
N5	H5B	O10[6]	0.91	1.86	2.750(6)	164.1
N6	H6A	O1	0.91	1.83	2.733(6)	169.7
N6	H6B	O2[7]	0.91	1.90	2.769(6)	160.0

[1]-1+x,1+y,+z; [2]1+x,-1+y,+z; [3]1+x,-1+y,1+z; [4]-1+x,+y,1+z; [5]1+x,+y,-1+z; [6]2-x,1-y,-z; [7]1-x,2-y,-z

Table S5. Atomic Occupancies for all atoms that are not fully occupied in $(Me_2NH_2)_2$[Pd(TPPP-A)$_{-2H}$].

Atom	Occupancy
C43A	0.734(10)
H43A	0.734(10)
C44A	0.734(10)
H44A	0.734(10)

Atom	Occupancy
C40A	0.734(10)
H40A	0.734(10)
C41A	0.734(10)
H41A	0.734(10)
C40	0.266(10)

Atom	Occupancy
H40	0.266(10)
C44	0.266(10)
H44	0.266(10)
C43	0.266(10)
H43	0.266(10)

Atom	Occupancy
C41	0.266(10)
H41	0.266(10)

Table S6. Solvent masking (PLATON/SQUEEZE) information for $(Me_2NH_2)_2$[Pd(TPPP-A)$_{-2H}$].

No	x	y	z	V	e	Content
1	-0.527	0.000	0.500	777.2	318.3	8C3H7NO

4. Electrochemical and spectroelectrochemical studies

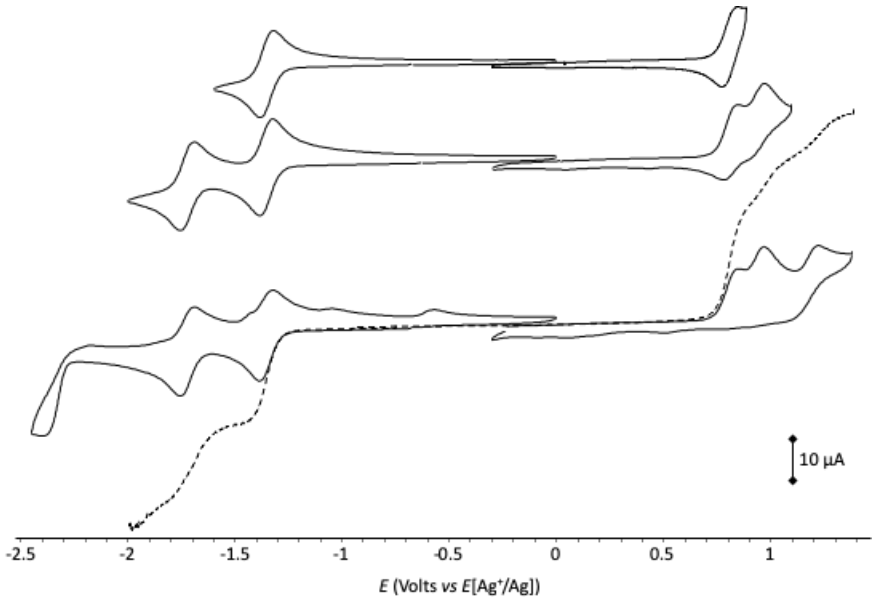

Figure S4. Cyclic voltamograms recorded with H_2(TPPP) (1mM in MeCN + TBAP (0.1 M), vitreous carbon working electrode (∅ = 3 mm), $\nu = 0.1$ V s^{-1}, *E vs* [Ag^+(0.01M)/Ag]).

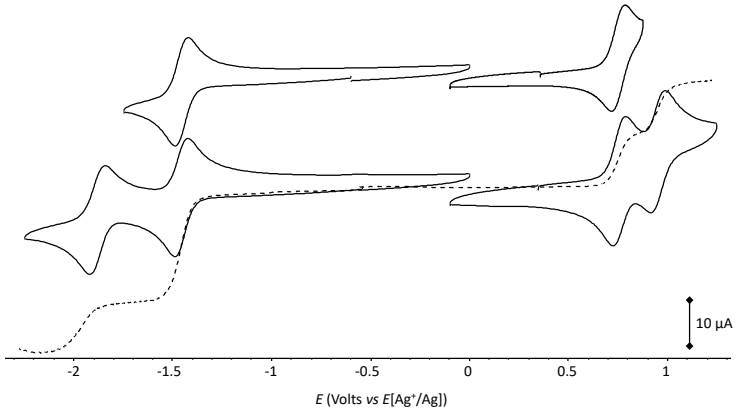

Figure S5. Cyclic voltamograms recorded with Cu(TPPP) (1mM in MeCN + TBAP (0.1 M), vitreous carbon working electrode (∅ = 3 mm), $\nu = 0.1$ V s^{-1}, *E vs* [Ag^+(0.01M)/Ag]).

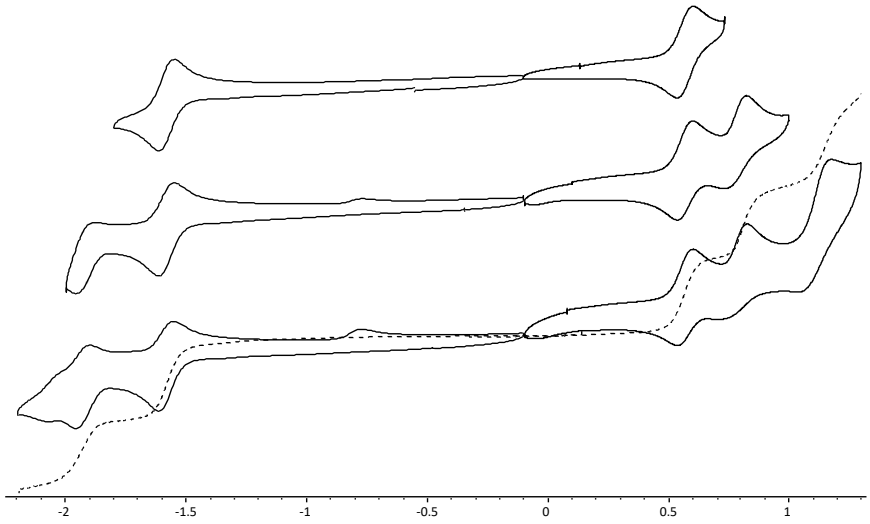

Figure S6. Cyclic voltamograms recorded with Zn(TPPP) (1mM in MeCN + TBAP (0.1 M), vitreous carbon working electrode (∅ = 3 mm), $\nu = 0.1$ V s^{-1}, *E vs* [Ag^{+}(0.01M)/Ag]).

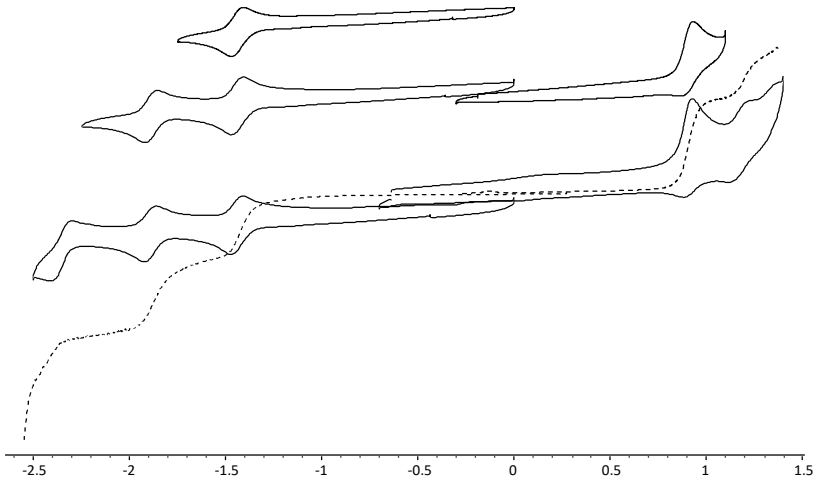

Figure S7. Cyclic voltamograms recorded with Pd(TPPP) (1mM in MeCN + TBAP (0.1 M), vitreous carbon working electrode (∅ = 3 mm), $\nu = 0.1$ V s^{-1}, *E vs* [Ag^{+}(0.01M)/Ag]).

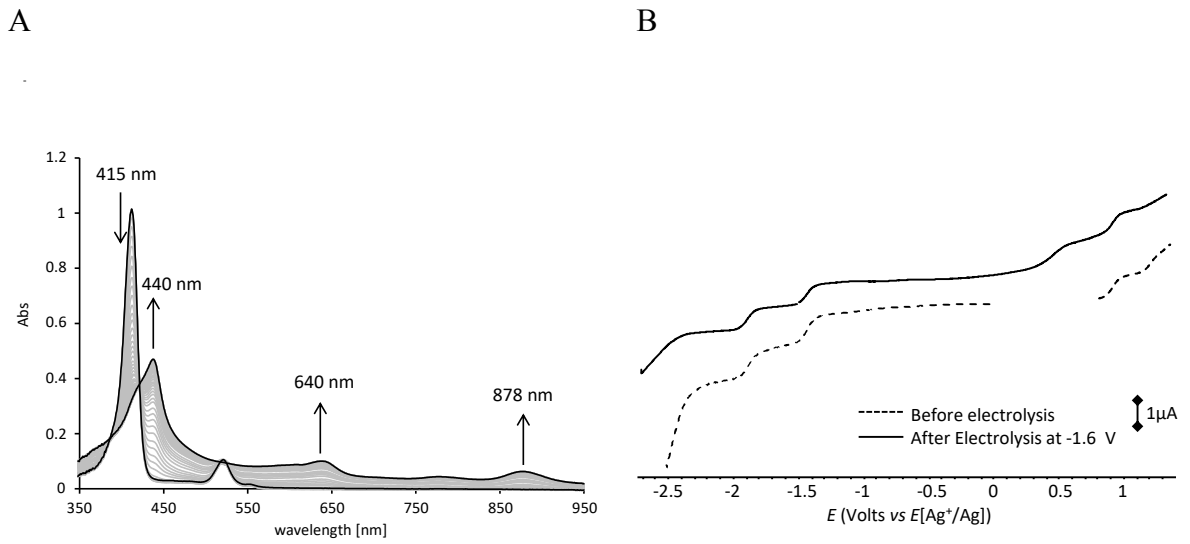

Figure S8. (A) UV–vis–NIR spectra recorded during the exhaustive one-electron reduction of Pd(TPPP) ($2.4 \cdot 10^{-5}$ M) in MeCN (0.1 M TBAP, working electrode: Pt, 10 mL, E_{app}= –1.6 V, l = 1 mm, $t \approx 30$ min). (B) Rotatory disk electrode measurements carried out before (dashed line) and after (solid line) the first one-electron reduction of Pd(TPPP) at E_{app} = –1.6 V (RDE, 10 m·s^{-1}, 500 r/min).

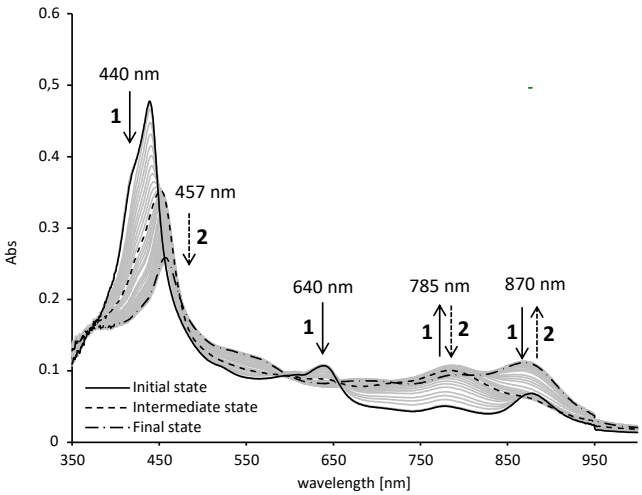

Figure S9. UV–vis–NIR spectra recorded during two consecutive reductions waves of Pd(TPPP) ($2.4 \cdot 10^{-5}$ M) in MeCN (0.1 M TBAP, working electrode: Pt, 10 mL, E_{app}= –2.15 V, l = 1 mm, $t \approx 30$ min).

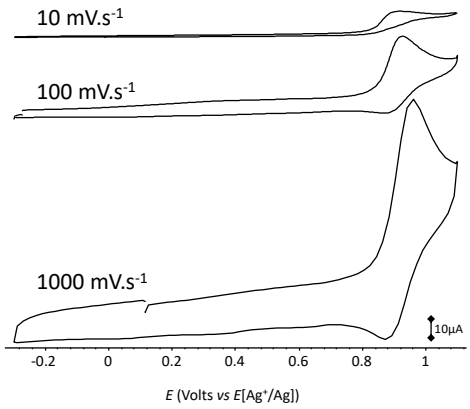

Figure S10. Cyclic voltamograms of Pd(TPPP) recorded at 10, 100 and 1000 mV s^{-1}(1mM in MeCN + TBAP (0.1 M), vitreous carbon working electrode (∅ = 3 mm), *E vs* [Ag^+(0.01M)/Ag]).

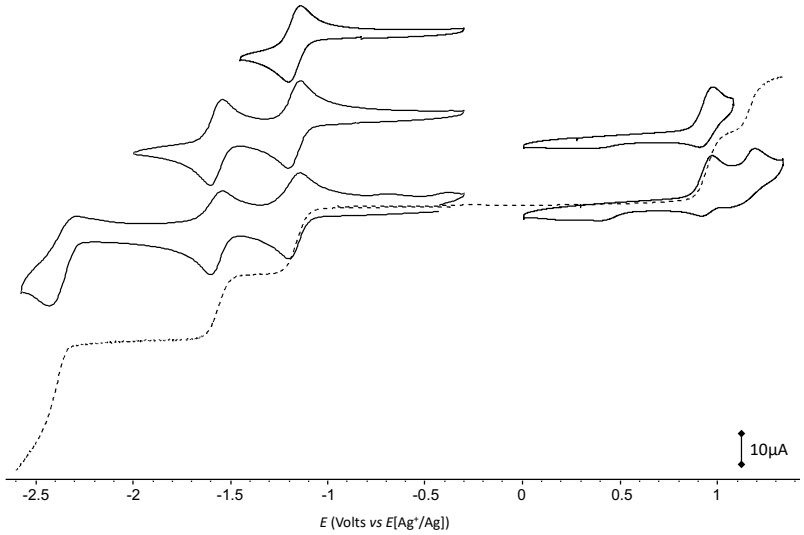

Figure S11. Cyclic voltamograms recorded with In(TPPP) (1mM in MeCN + TBAP (0.1 M), vitreous carbon working electrode (∅ = 3 mm), v = 0.1 V s^{-1}, *E vs* [Ag^+(0.01M)/Ag]).

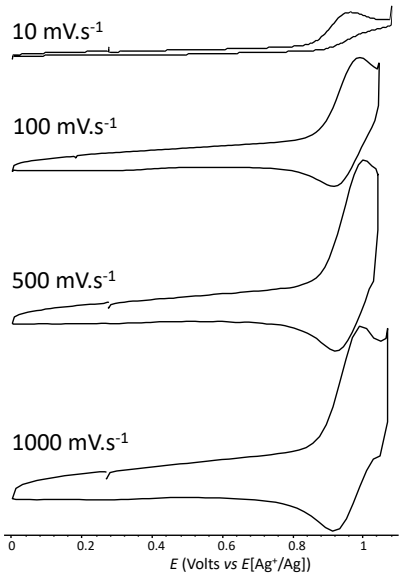

Figure S12. Cyclic voltamograms of In(TPPP) recorded at 10, 100, 500 and 1000 mV s^{-1} (1mM in MeCN + TBAP (0.1 M), vitreous carbon working electrode (∅ = 3 mm), *E vs* [Ag^+(0.01M)/Ag]).

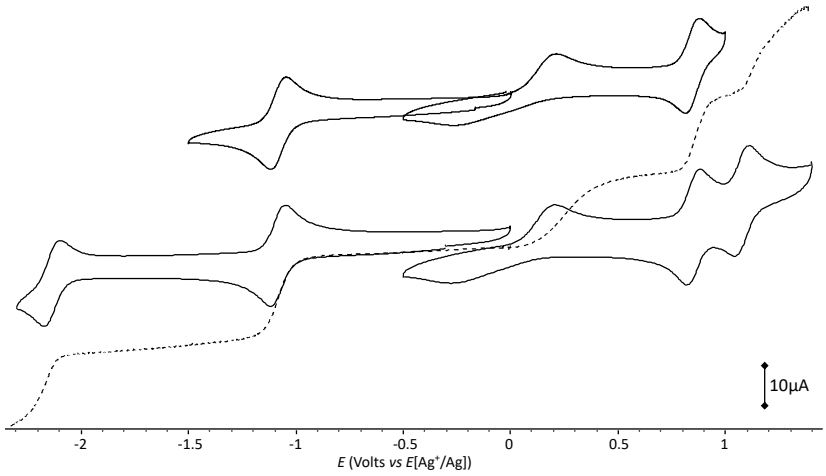

Figure S13. Cyclic voltamograms recorded with Co(TPPP) (1mM in MeCN + TBAP (0.1 M), vitreous carbon working electrode (∅ = 3 mm), v = 0.1 V s^{-1}, *E vs* [Ag^+(0.01M)/Ag]).

5. Studies of optical properties

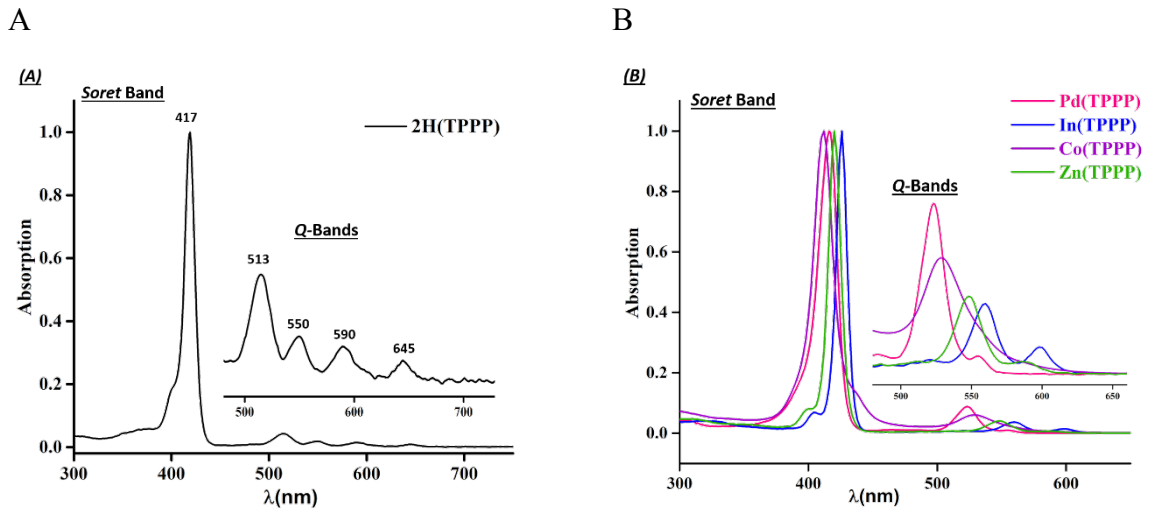

Figure S14. UV–vis spectra of H_2(TPPP) (A) and M(TPPP) (M = Zn, Pd, Co and In) (B) in dichloromethane (c = 1 μM) at room temperature.

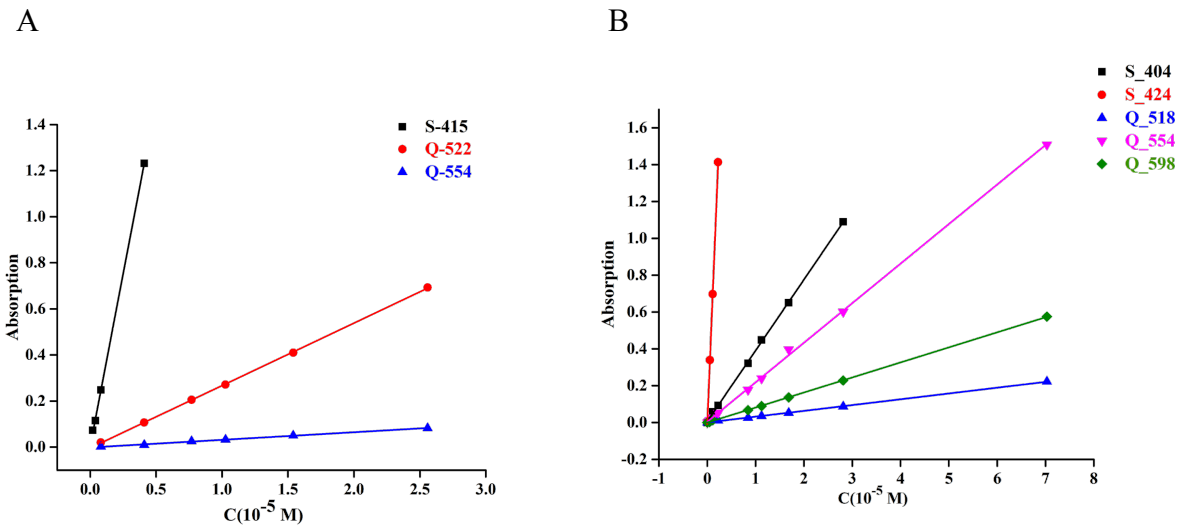

Figure S15. Beer-Lambert's law plots for Pd(TPPP) (A) and In(TPPP) (B) in CH_2Cl_2 at room temperature for different absorption bands. The corresponding λ_{max} values are indicated in the legend.

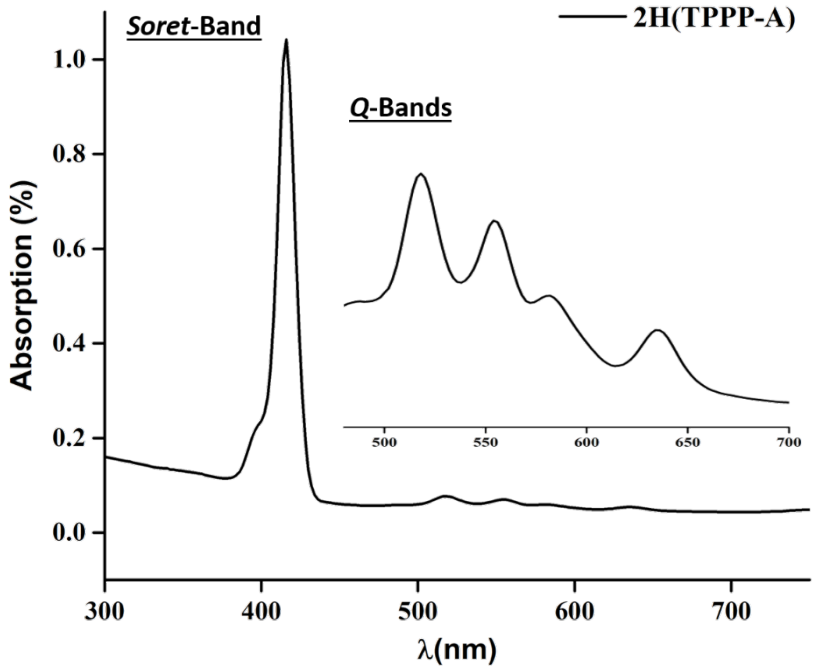

Figure S16. UV–vis spectrum of H_2(TPPP-A) in water (c = 1 μM, 1 drop of 0.1 M NaOH).

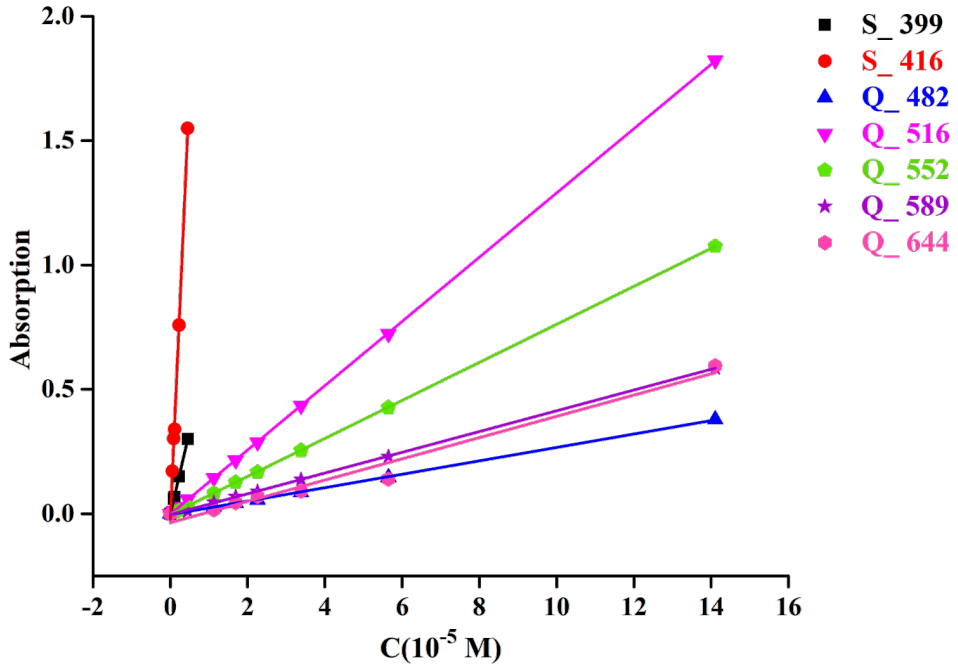

Figure S17. Beer-Lambert's law plots for H_2(TPPP-A) in water (c = 1 μM, 1 drop of 0.1 M NaOH). The corresponding λ_{max} values are indicated in the legend.

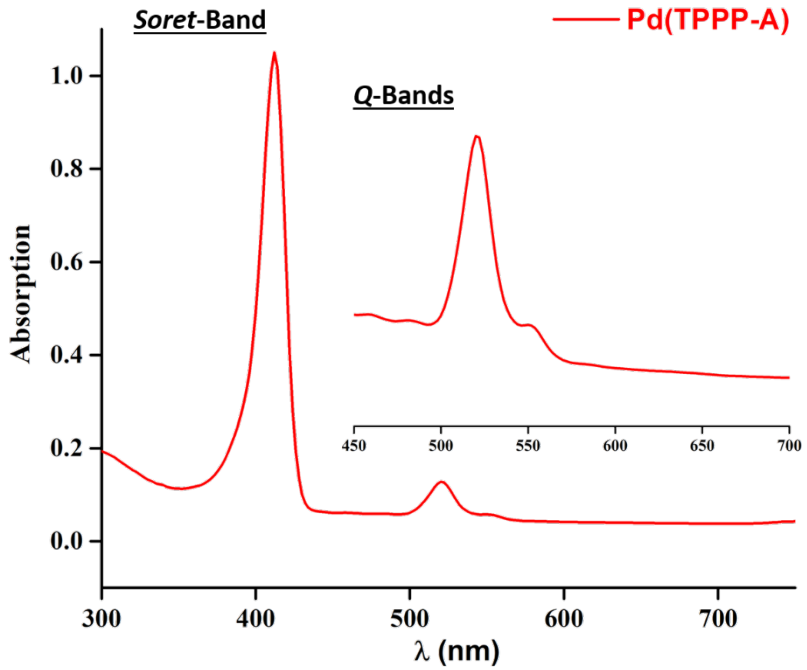

Figure S18. UV–vis spectrum of Pd(TPPP-A) in water (c = 1 μM, 1 drop of 0.1 M NaOH).

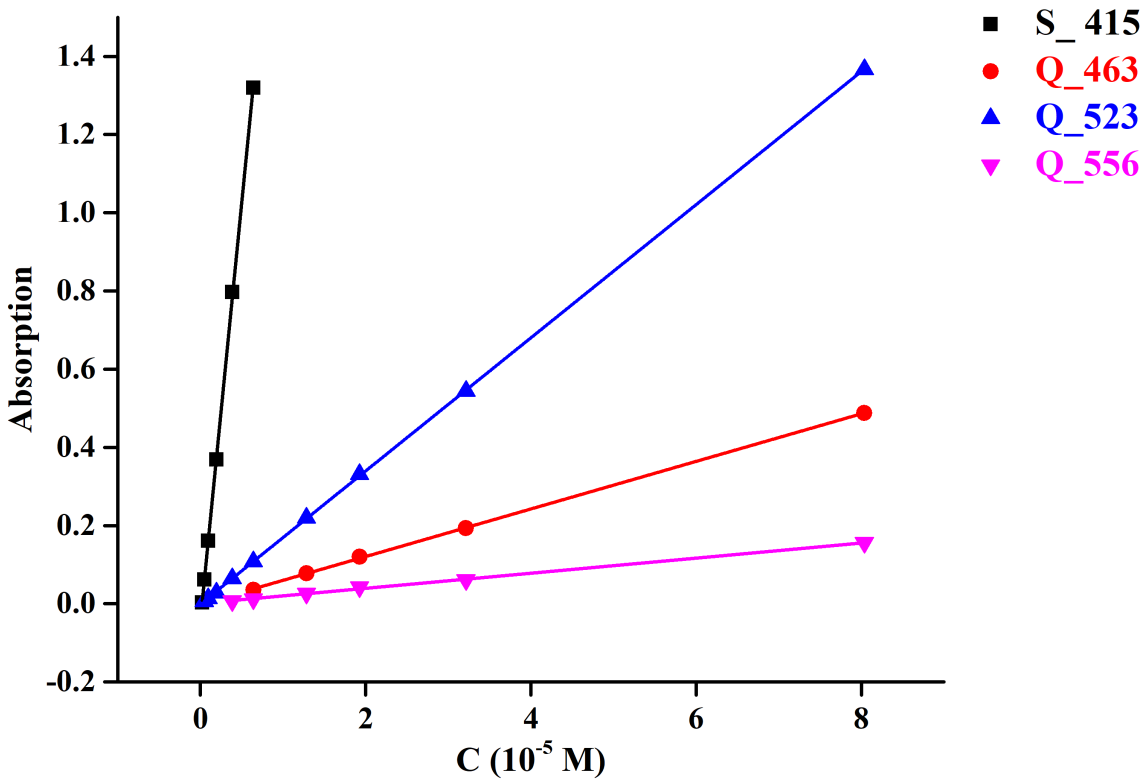

Figure S19. Beer-Lambert's law plots for Pd(TPPP-A) in MeCN/H_2O (1:1 v/v; c = 0.01 mM).at room temperature. The corresponding λ_{max} values are indicated in the legend.

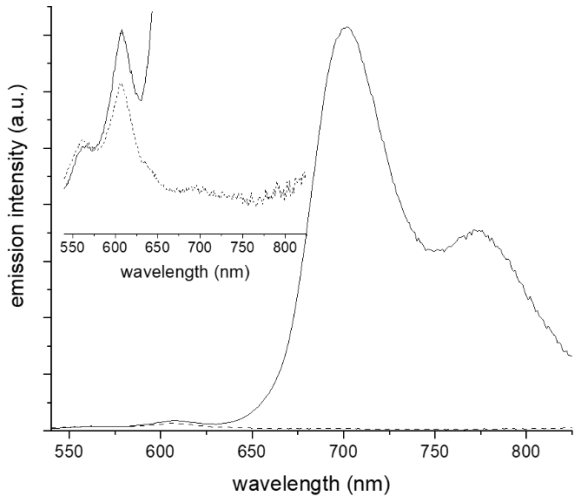

Figure S20. Emission spectra (solid for deoxygenated sample and dashed for oxygen-containing sample) for Pd(TPPP-A) in basified MeCN/H_2O (1:1 v/v) solution.

6. Photostability studies

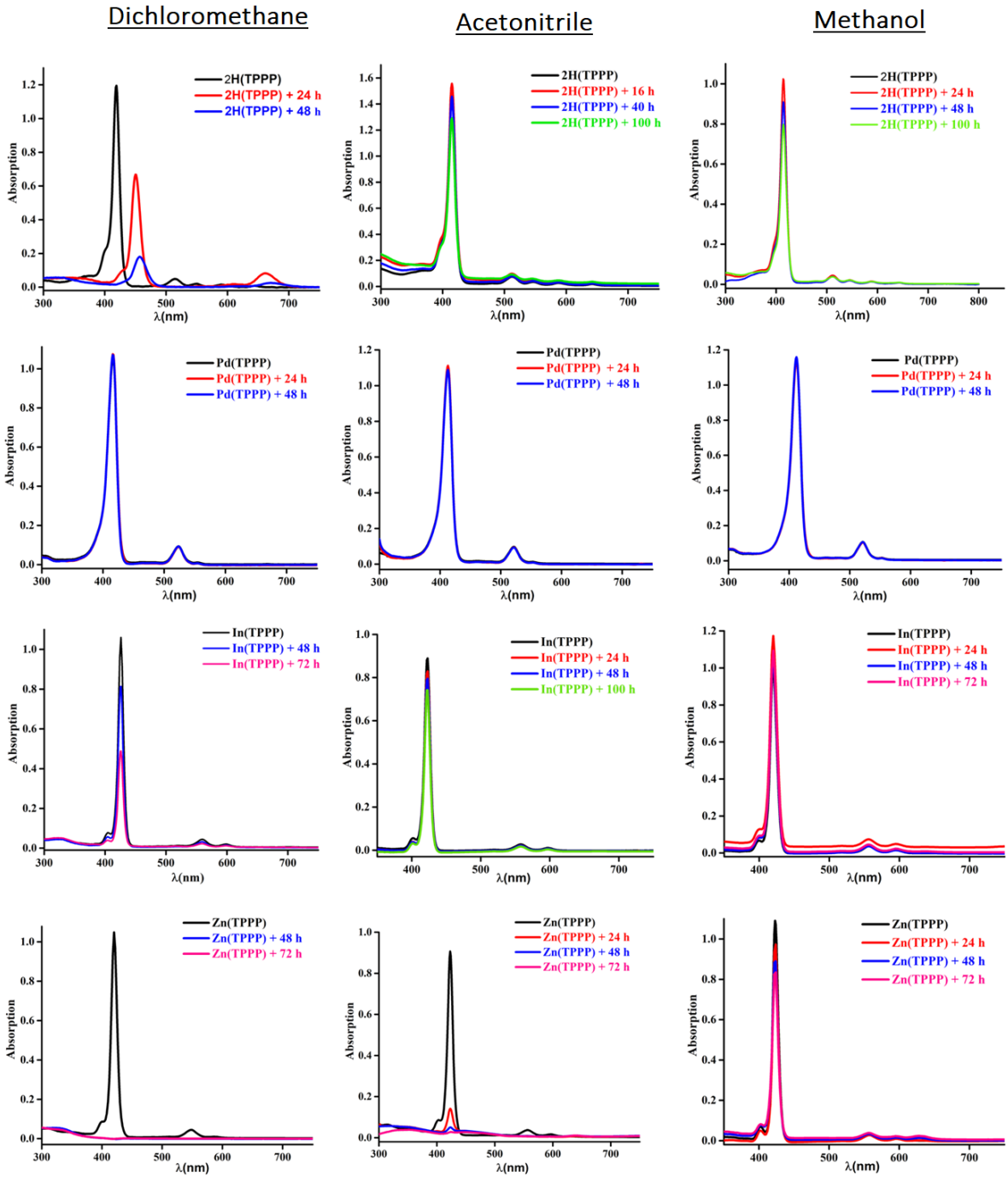

Figure S21. Evolution of the UV-vis spectra of H_2(TPPP), Pd(TPPP), In(TPPP), and Zn(TPPP) in dichloromethane, acetonitrile, and methanol under irradiation with a blue LED (3 W).

7. Studies on the single oxygen generation

The photophysical measurements were carried out in CD_3CN/D_2O (10:1 v/v) by direct detection of the singlet oxygen phosphorescence signal at 1270 nm. Deuterated solvents were chosen here, as they ensure that singlet oxygen lifetime is long enough to enable detection and quantitative evaluation of its phosphorescence signal with enough accuracy and high signal-to-noise ratio. Measurements were performed upon irradiation in the Soret band of porphyrins (at *ca* 415 nm), first to match the conditions of the catalytic experiments, all performed under blue light irradiation, second to enable a systematic comparison with phenalen-1-one (perinaphtenone, **PH**) which was used as a standard.

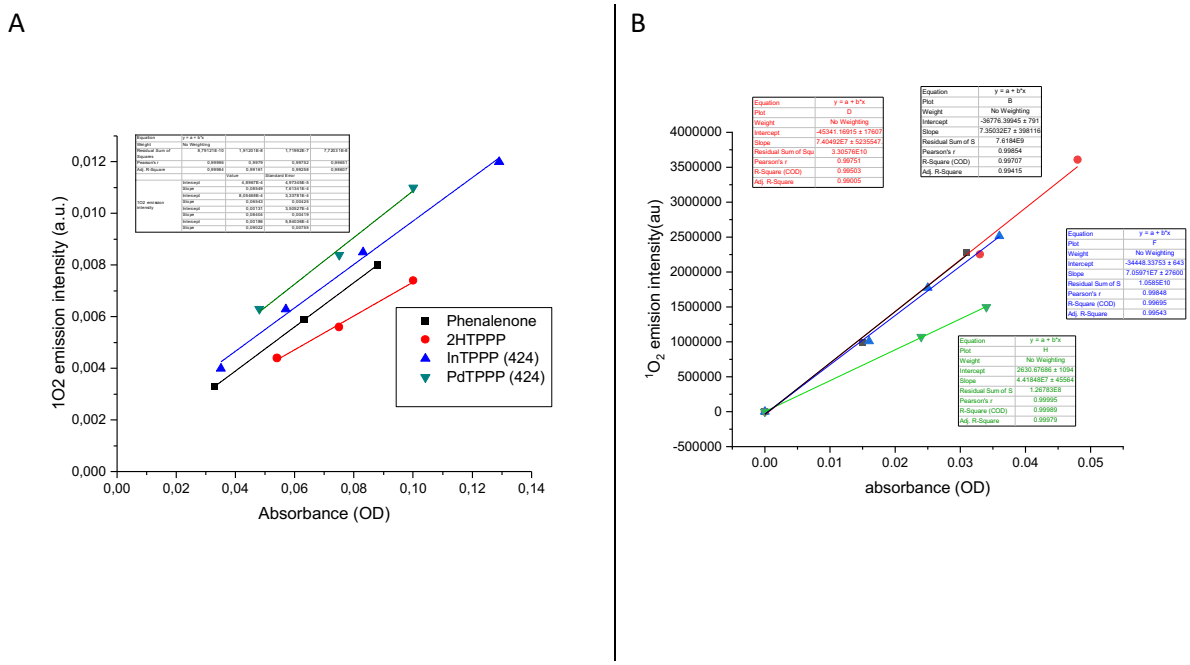

Figure S22. (A) Plot of the $^1O_2$ emission intensity vs absorbance of CD_3CN/D_2O solutions for phenalen-1-one (**PH**) (black squares), H_2(TPPP) (red circles) In(TPPP) (blue triangles) and Pd(TPPP) (green triangles). Linear fits, with the respective color code. (B) Plot of the $^1O_2$ emission intensity vs absorbance of $CDCl_3$ solutions for phenalenone (black squares) PdTPPP (red circles) InTPPP (blue triangles) and H_2(TPPP) (green triangles). Linear fits, with the respective color code. Phenalenone taken as a reference (φ_Δ =0.97 in chloroform) gives values for PdTPPP φ_Δ =0.97; for InTPPP φ_Δ =0.93; for H_2(TPPP) φ_Δ =0.58).

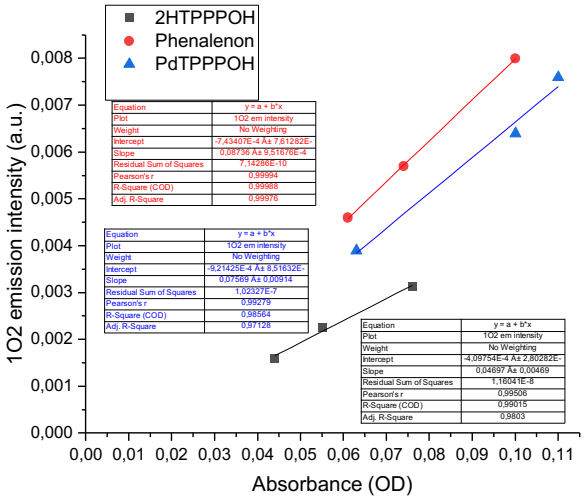

Figure S23. Plot of the $^1O_2$ emission intensity vs absorbance of CD_3CN/D_2O (1:1 v/v) solutions for phenalen-1-one (**PH**) (red circles), H_2(TPPP) (black squares) and Pd(TPPP) (blue triangles). Linear fits, with the respective color code.

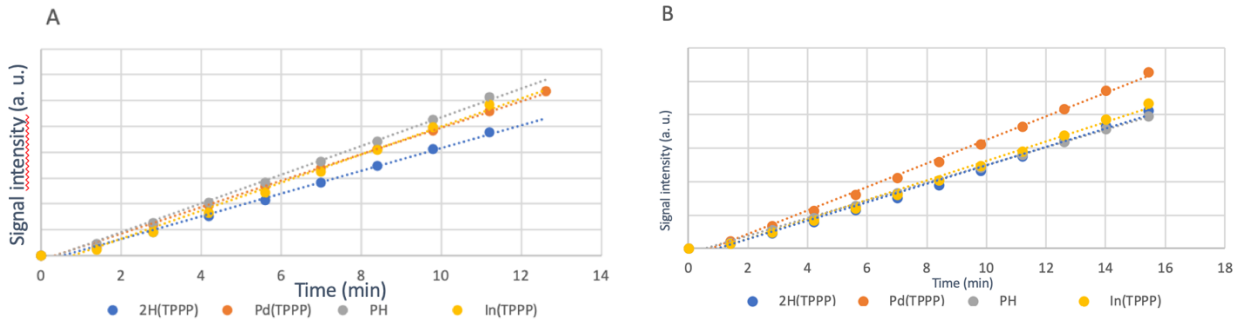

Figure S24. Kinetics of TEMPO generation in the presence of H_2(TPPP), Pd(TPPP), In(TPPP) and phenalen-1-one (**PH**) in MeCN (A) and MeCN–H_2O (10:1 v/v) solutions (B).

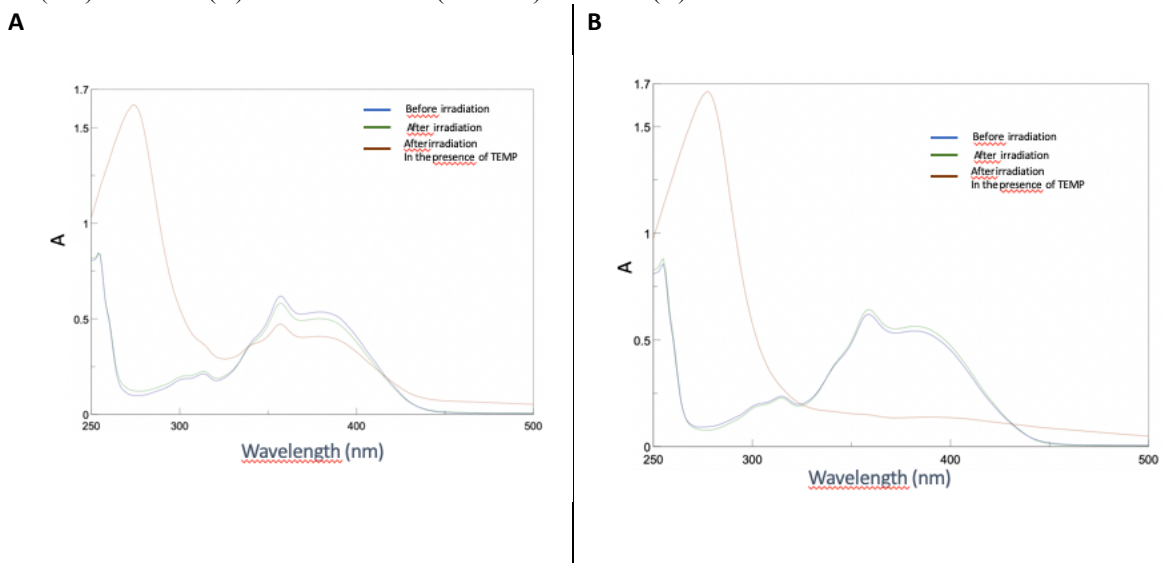

Figure S25. UV–vis absorption spectra of phenalen-1-one (**PH**) in MeCN (A) and MeCN/H_2O (10:1 v/v) (B) before and after irradiation at 365 nm (EvoluChem®, 30 W, AC-200) in HepatoChem® photoreactor for 1 h in the presence and in the absence of TEMP.

8. DFT calculations

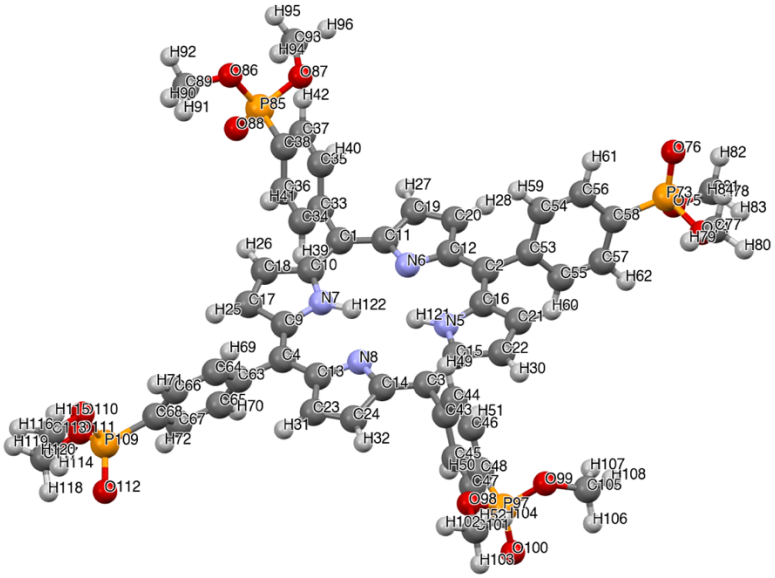

Figure S26. The structure of H_2(TPPP-Me) complex obtained by full geometry optimization at B3LYP/Jorge-DZP level.

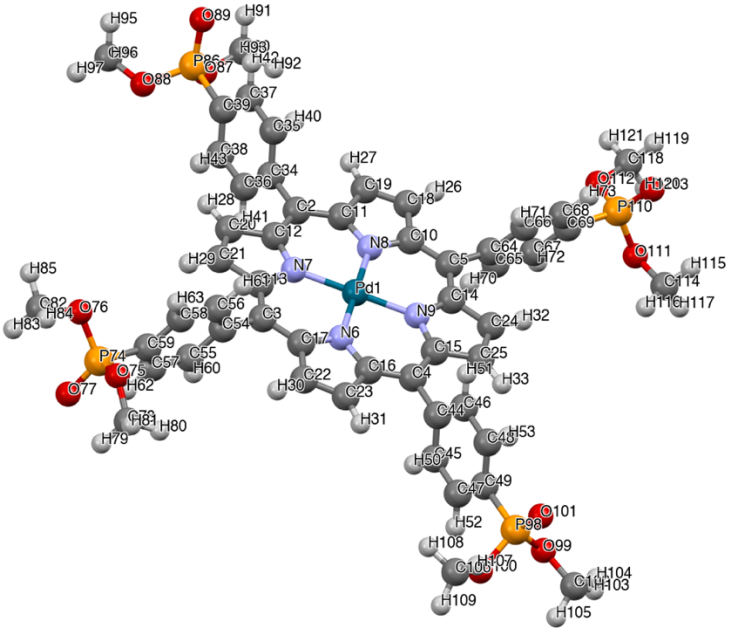

Figure S27. The structure of Pd(TPPP-Me) complex obtained by full geometry optimization at B3LYP/Jorge-DZP level.

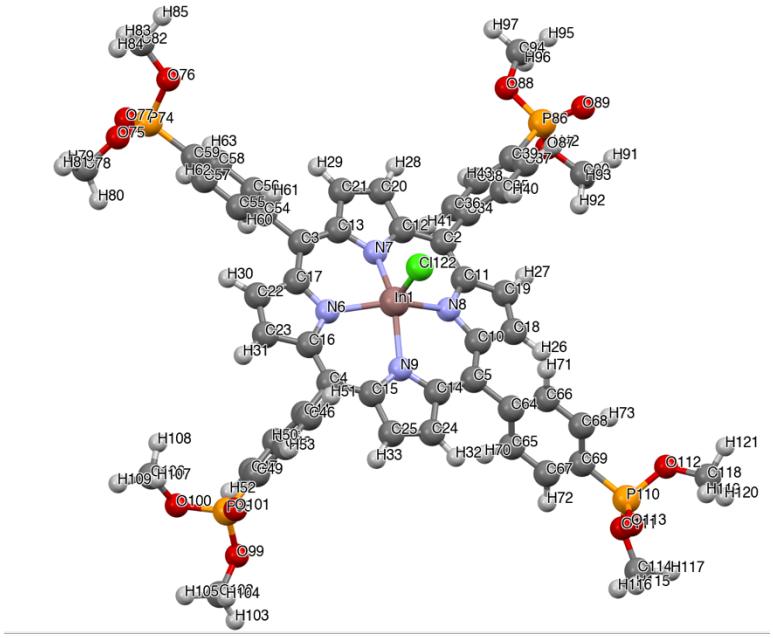

Figure S28. The structure of In(TPPP-Me) complex obtained by full geometry optimization at B3LYP/Jorge-DZP level.

Table S7. Selected bonds lengths (Å) and angles (°) in M(TPPP-Me) (M = H_2, Pd, In) obtained by full geometry optimization at B3LYP/Jorge-DZP level.

Compound	M–N	P=O	P–O	P–C	C–C(Ph)	N4–M[a]	N4/Ph dihedral angles
H_2(TPPP-Me)	-	1.500	1.630–1.648	1.811	1.397–1.406	-	70.54
							70.54
							71.48
							71.48
Pd(TPPP-Me)	1.980	1.500	1.630–1.648	1.812	1.397–1.406	0	76.98
							82.06
							84.60
							86.23
In(TPPP-Me)[b]	2.155–2.168	1.500	1.630-1.648	1.812	1.397–1.406	0.630	68.31
							74.39
							80.51
							80.51

[a] Deviation of metal atom from the mean plane of N atoms; [b] In–Cl = 2.372 Å.

9. Spectral characterization of M(TPPP) and M(TPPP-A)

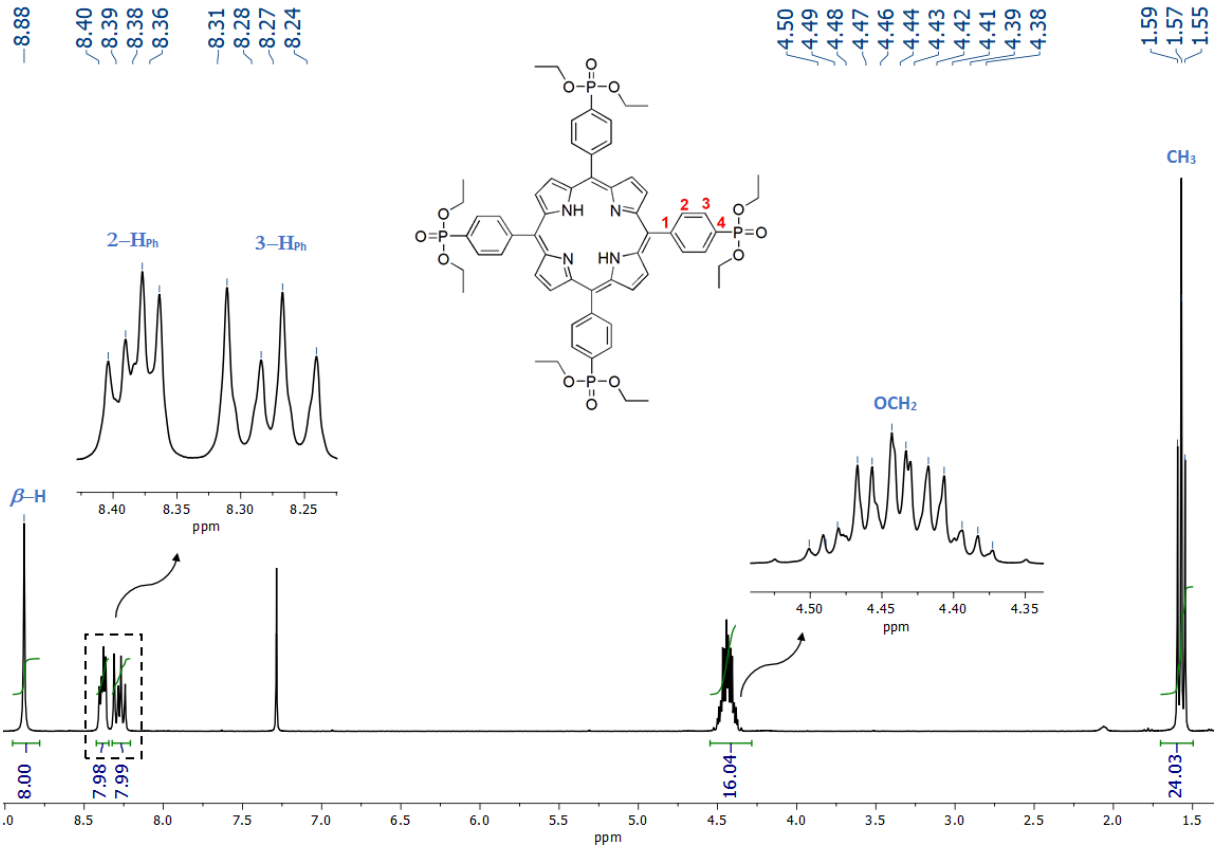

Figure S29. ^{1}H NMR spectrum of H_2(TPPP) (300 MHz, $CDCl_3$, 298 K).

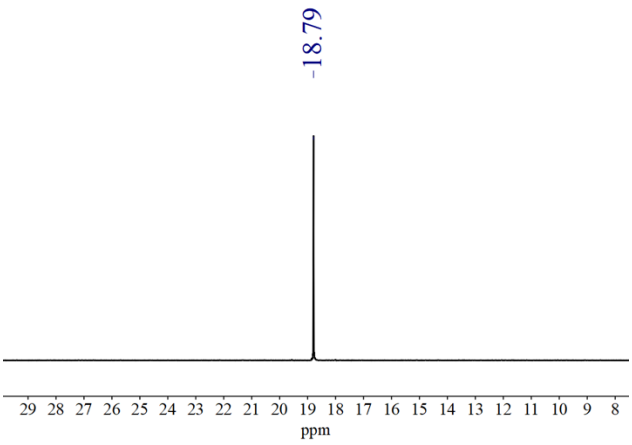

Figure S30. $^{31}P\{^{1}H\}$ NMR spectrum of H_2(TPPP) (121 MHz, $CDCl_3$, 298 K).

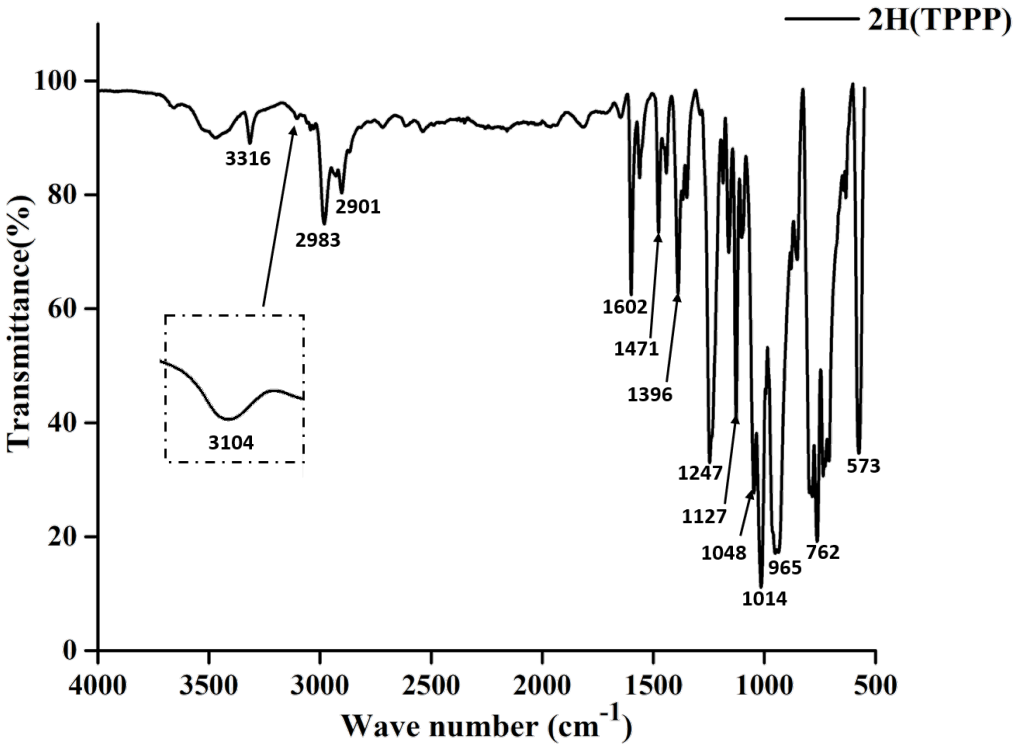

Figure S31. FT-IR spectrum of H_2(TPPP) (neat).

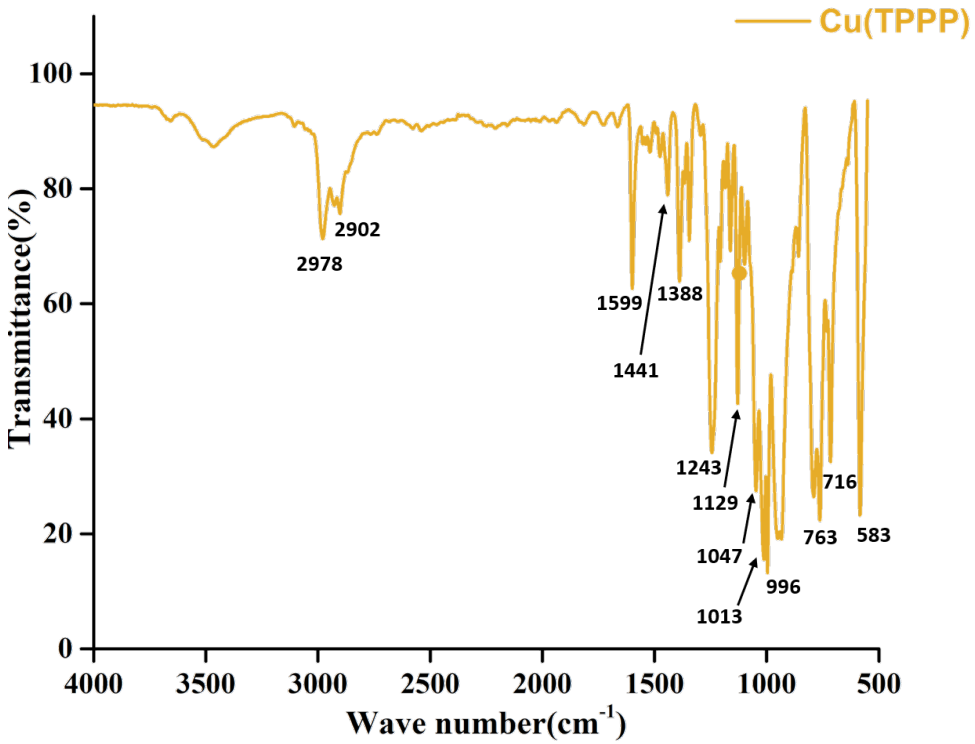

Figure S32. FT-IR spectrum of Cu(TPPP) (neat).

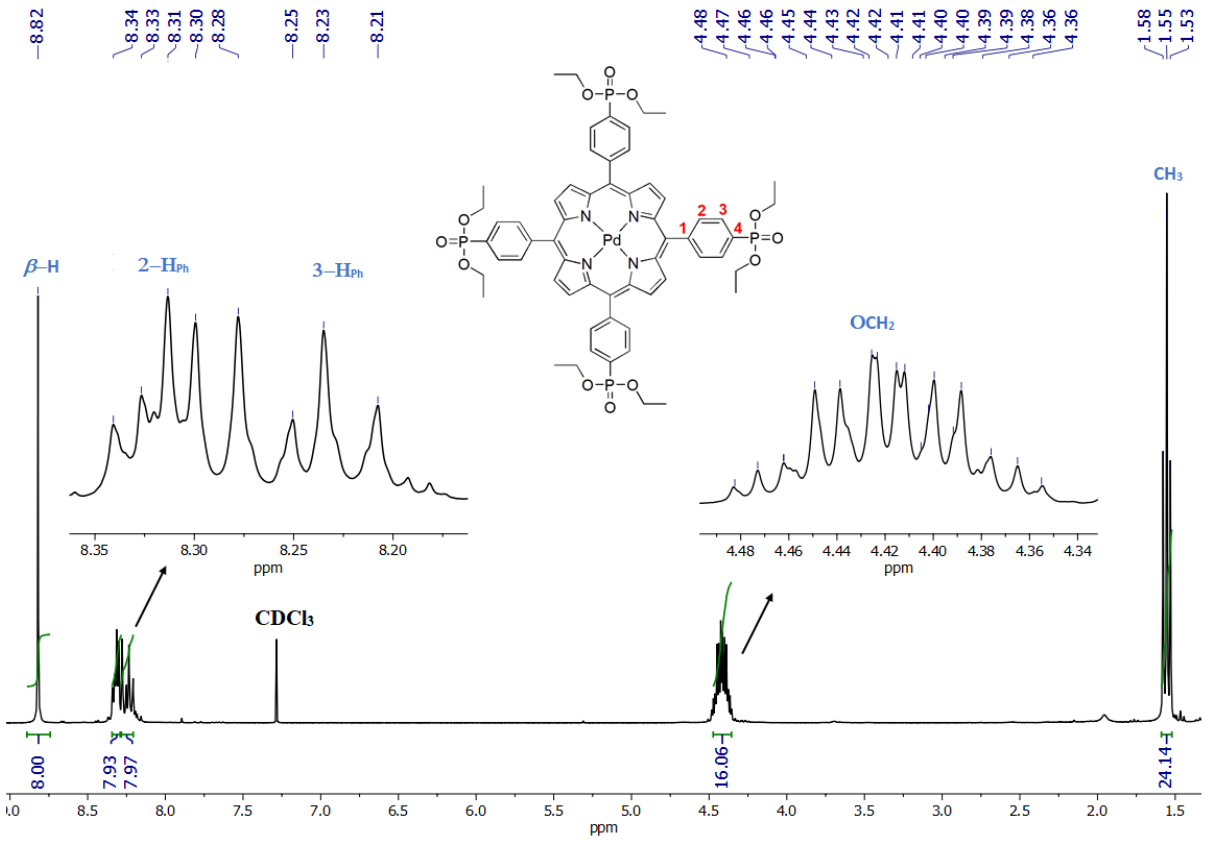

Figure S33. ^{1}H NMR spectrum of Pd(TPPP) (300 MHz, $CDCl_3$, 298 K).

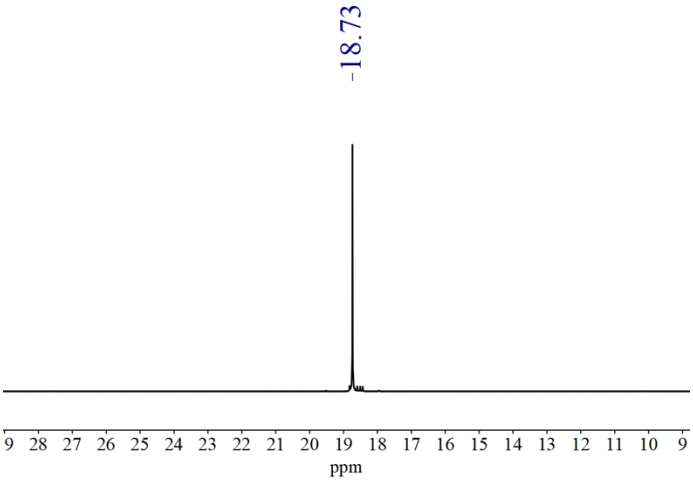

Figure S34. $^{31}P\{^{1}H\}$ NMR spectrum of Pd(TPPP) (121 MHz, $CDCl_3$, 298 K).

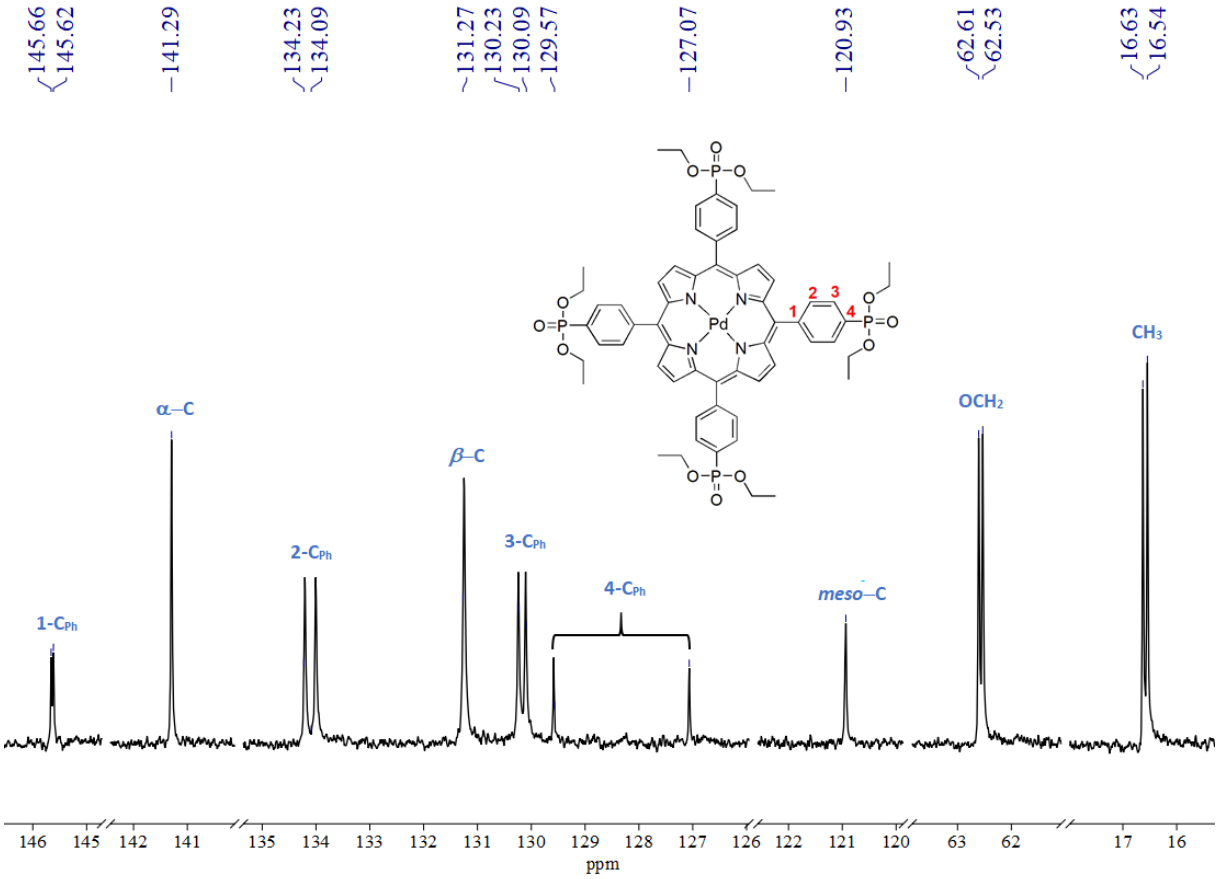

Figure S35. $^{13}C\{^{1}H\}$ NMR spectrum of Pd(TPPP) (75 MHz, $CDCl_3$, 298 K).

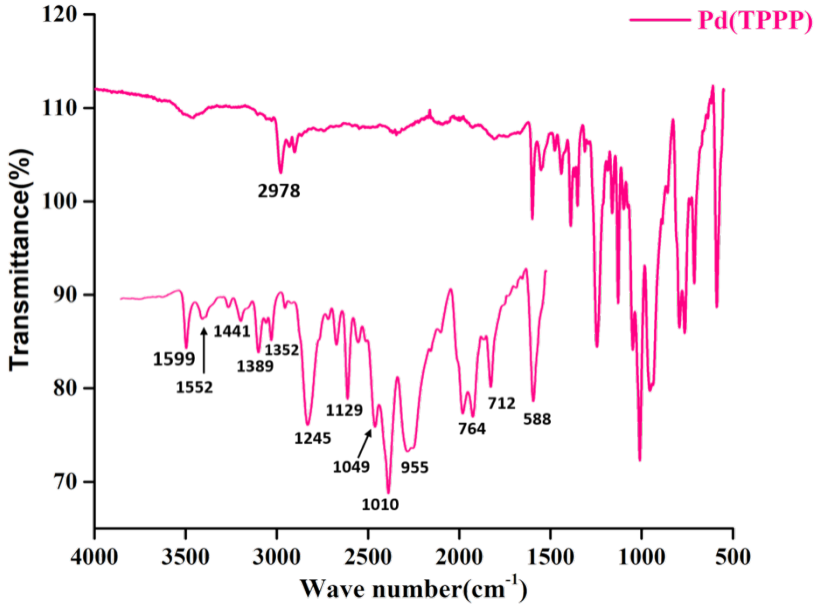

Figure S36. FT-IR spectrum of Pd(TPPP) (neat).

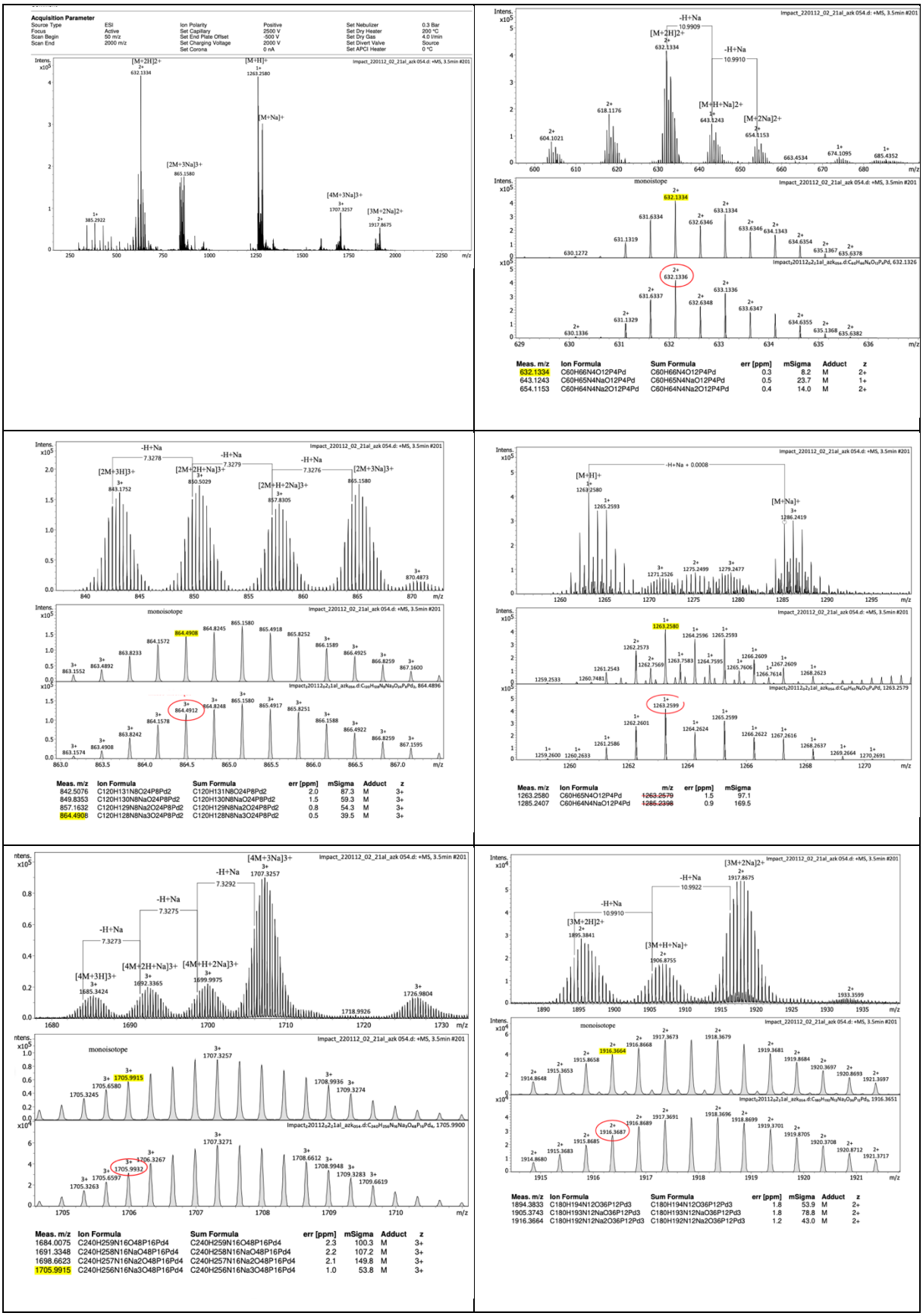

Figure S37. HRMS (ESI) spectrum of Pd(TPPP).

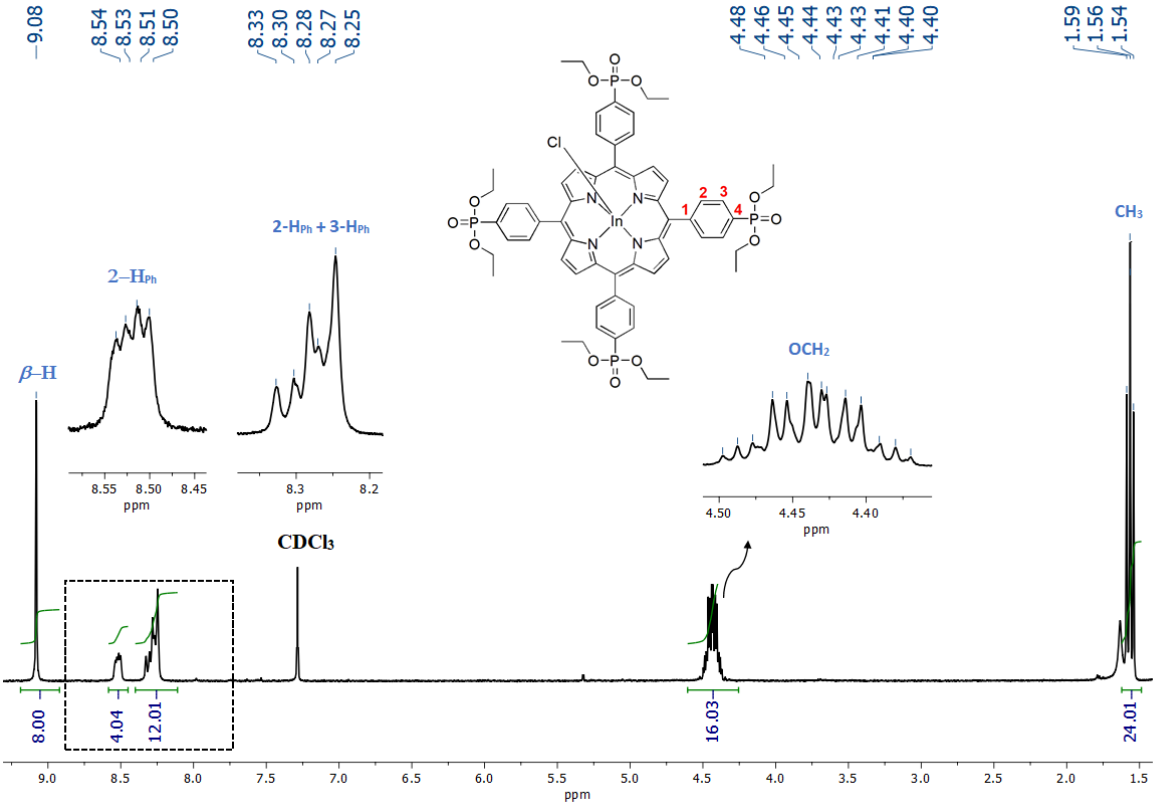

Figure S38. ^{1}H NMR spectrum of In(TPPP) (300 MHz, $CDCl_3$, 298 K).

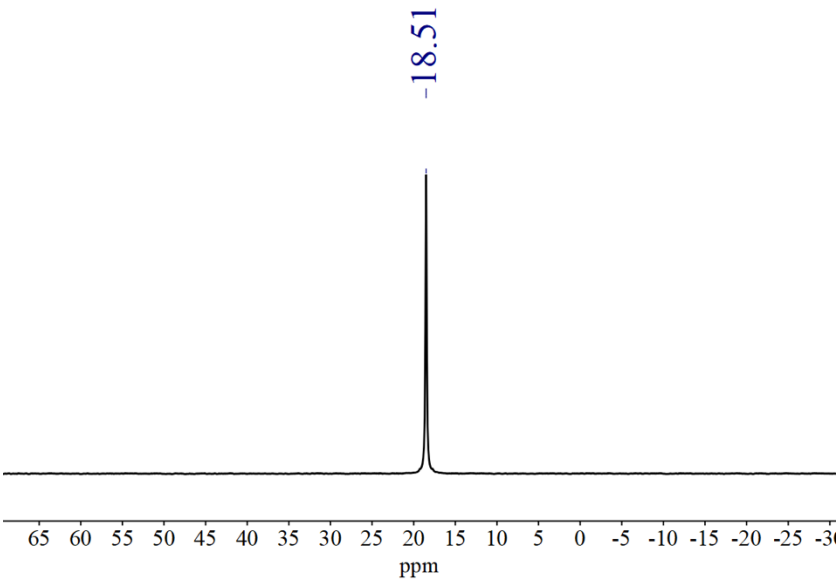

Figure S39. $^{31}P\{^{1}H\}$ NMR spectrum of In(TPPP) (121 MHz, $CDCl_3$, 298 K).

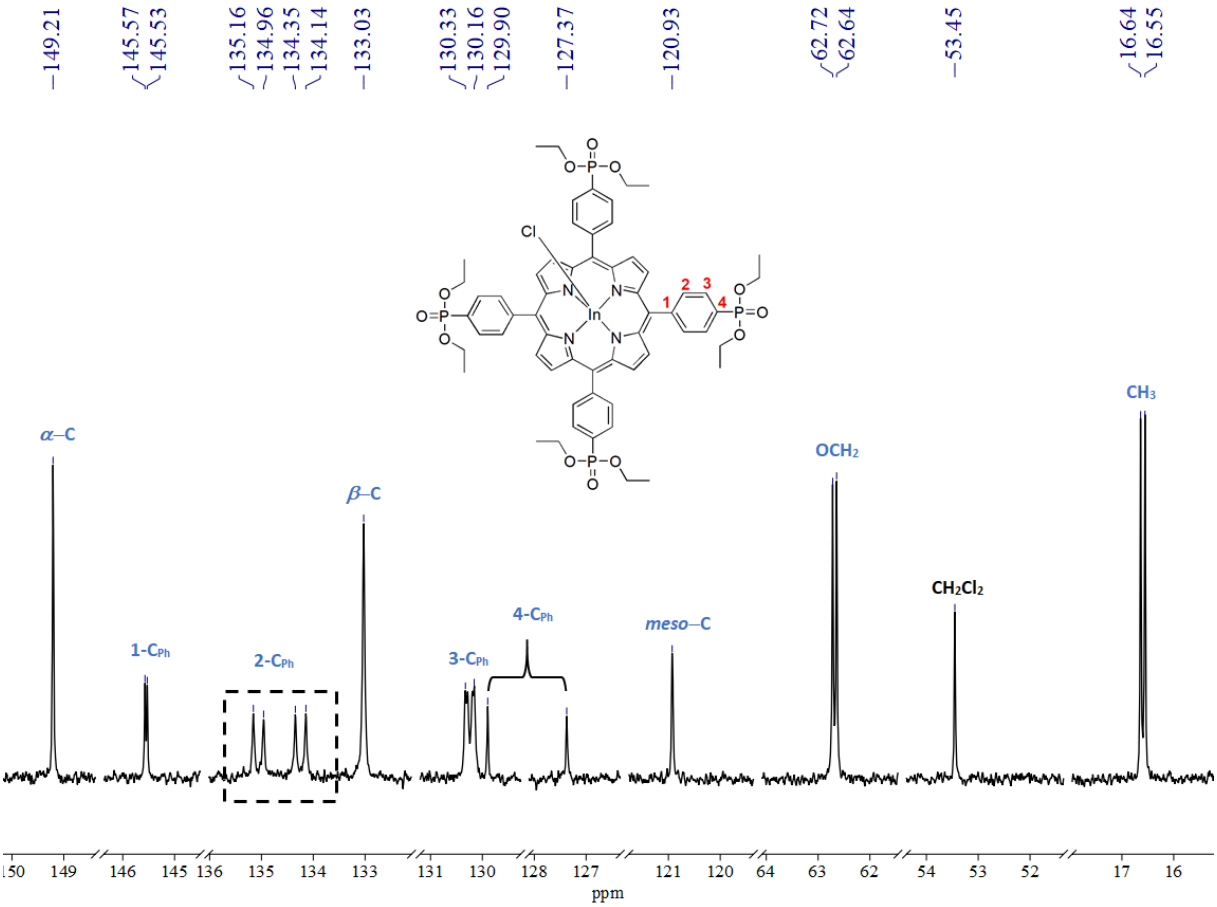

Figure S40. $^{13}C\{^{1}H\}$ NMR spectrum of In(TPPP) (75 MHz, $CDCl_3$, 298 K).

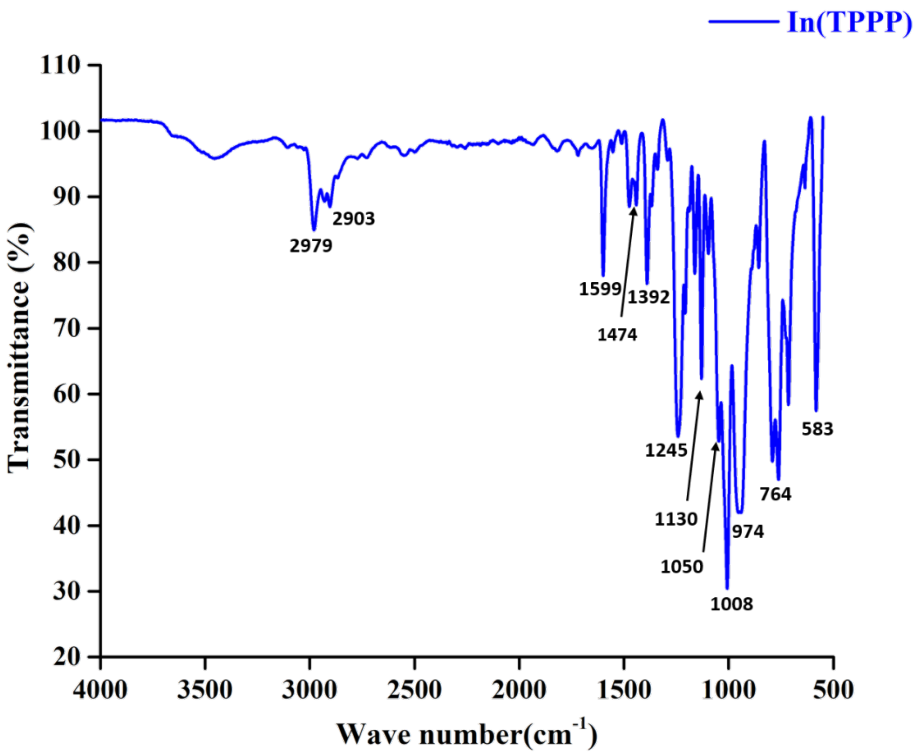

Figure S41. FT-IR spectrum of In(TPPP) (neat).

Acquisition Parameter

Source Type	ESI	Ion Polarity	Positive	Set Nebulizer	0.3 Bar
Focus	Active	Set Capillary	2500 V	Set Dry Heater	200 °C
Scan Begin	50 m/z	Set End Plate Offset	-500 V	Set Dry Gas	4.0 l/min
Scan End	2000 m/z	Set Charging Voltage	2000 V	Set Divert Valve	Source
		Set Corona	0 nA	Set APCI Heater	0 °C

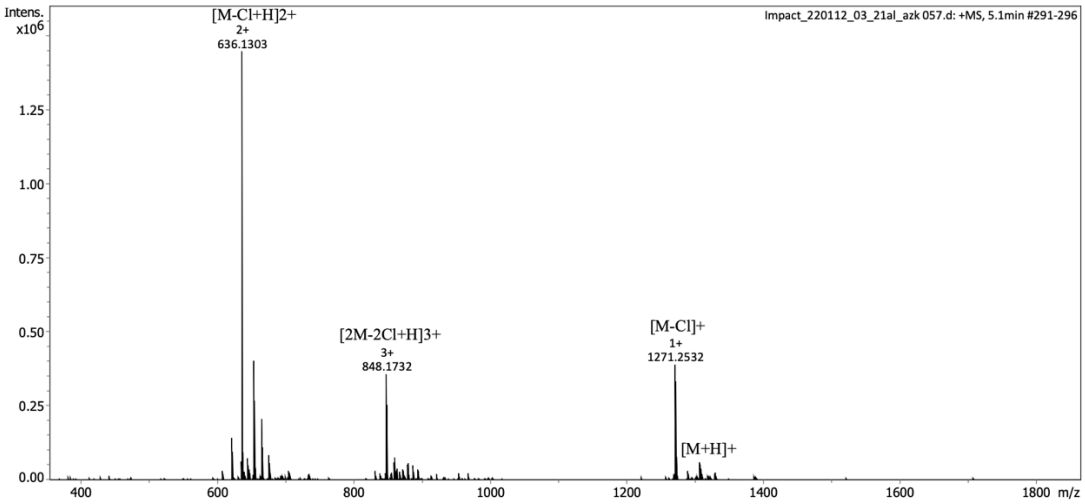

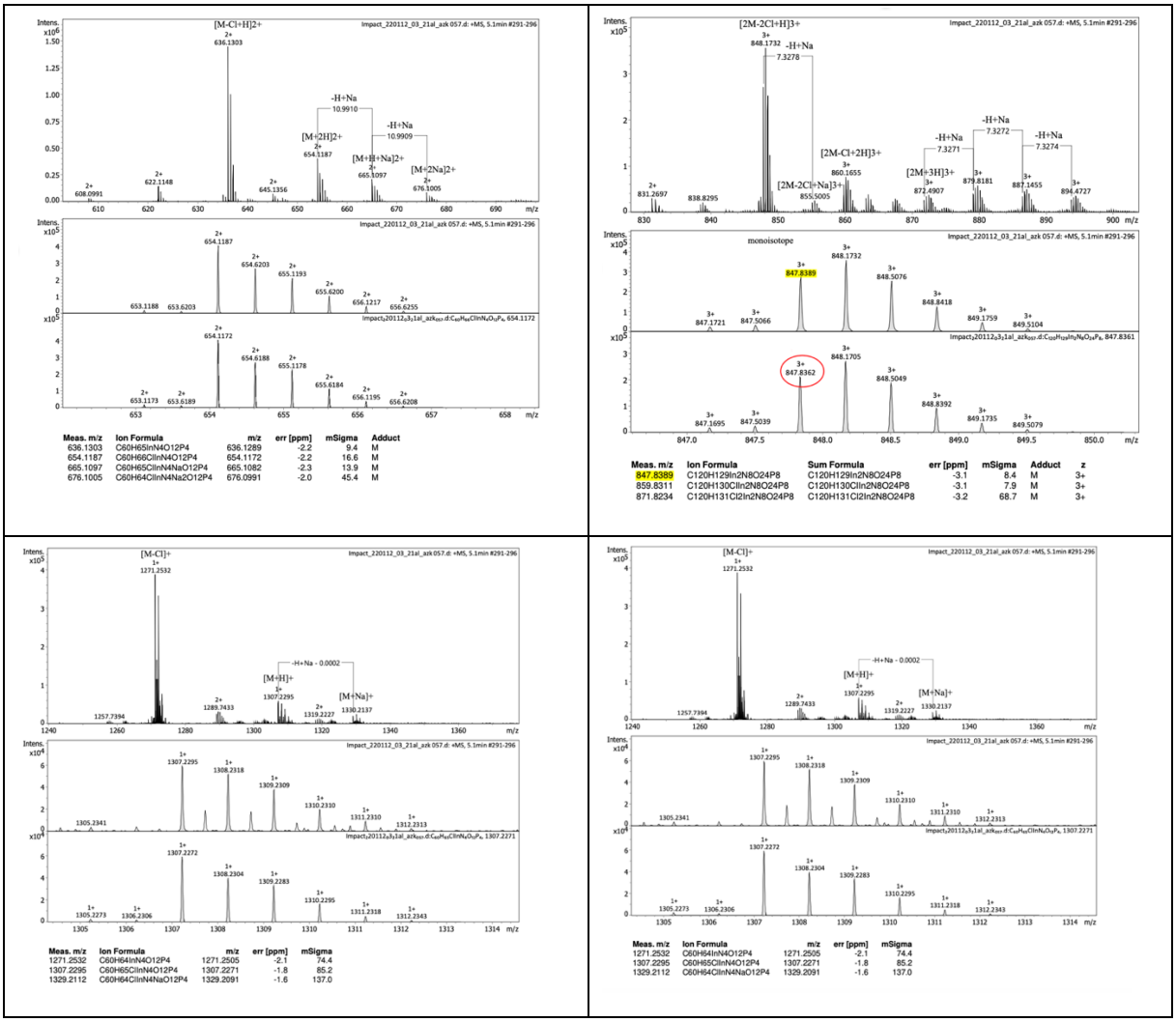

Figure S42. HRMS (ESI) spectrum of In(TPPP).

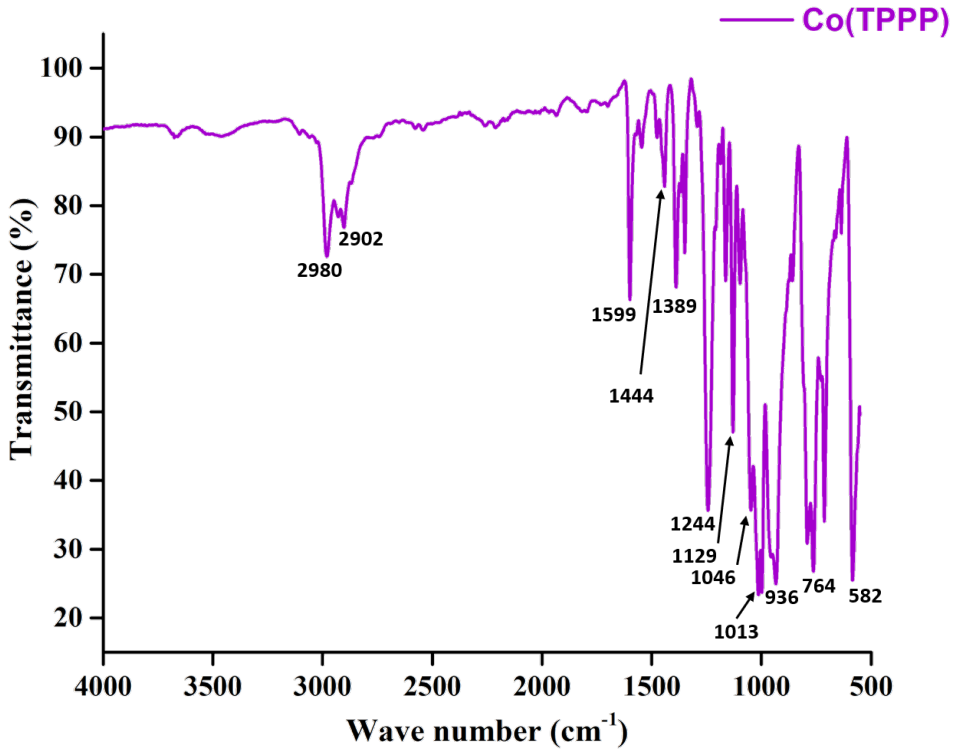

Figure S43. FT-IR spectrum of Co(TPPP) (neat).

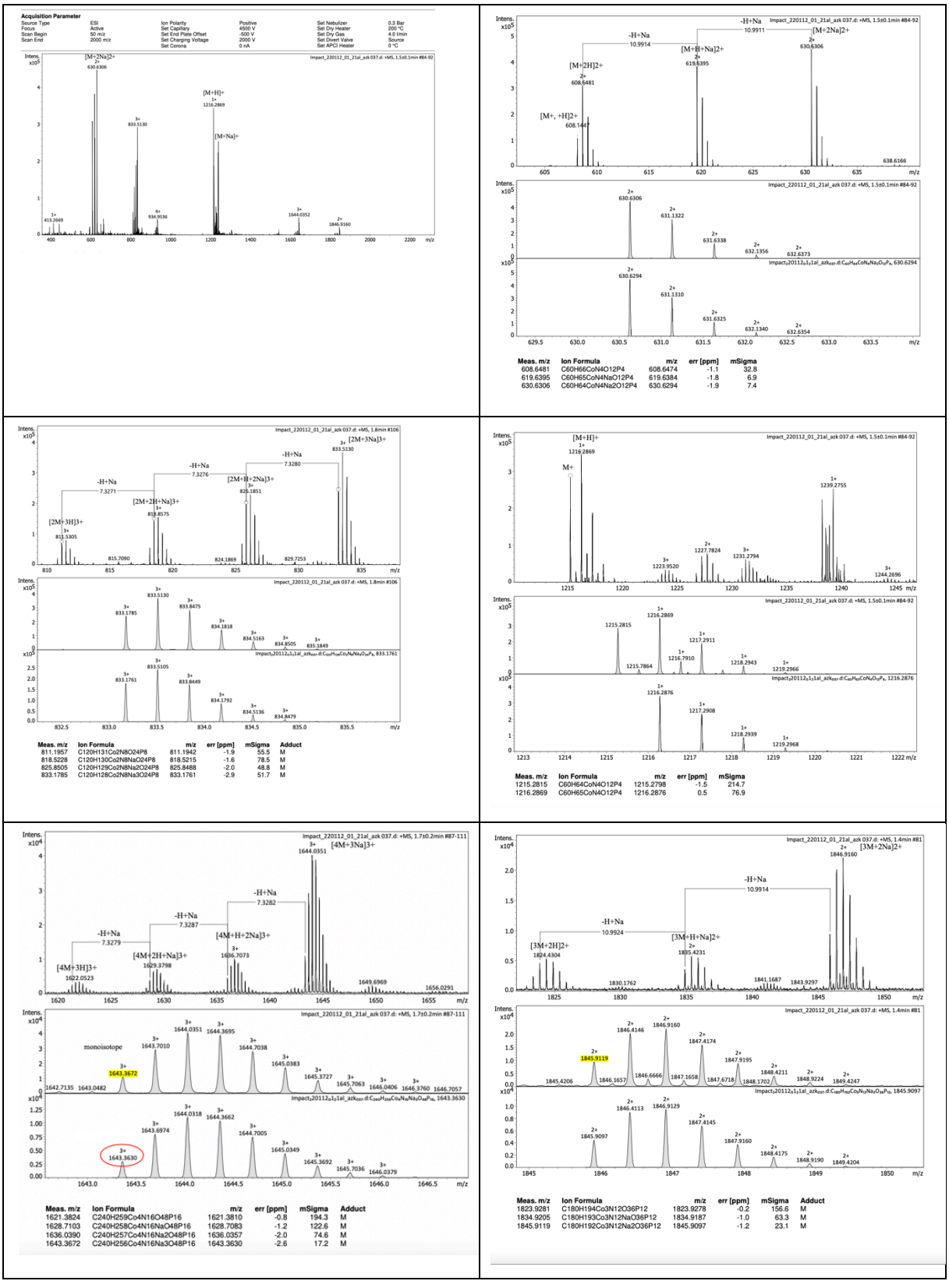

Figure S44. HRMS (ESI) spectrum of Co(TPPP).

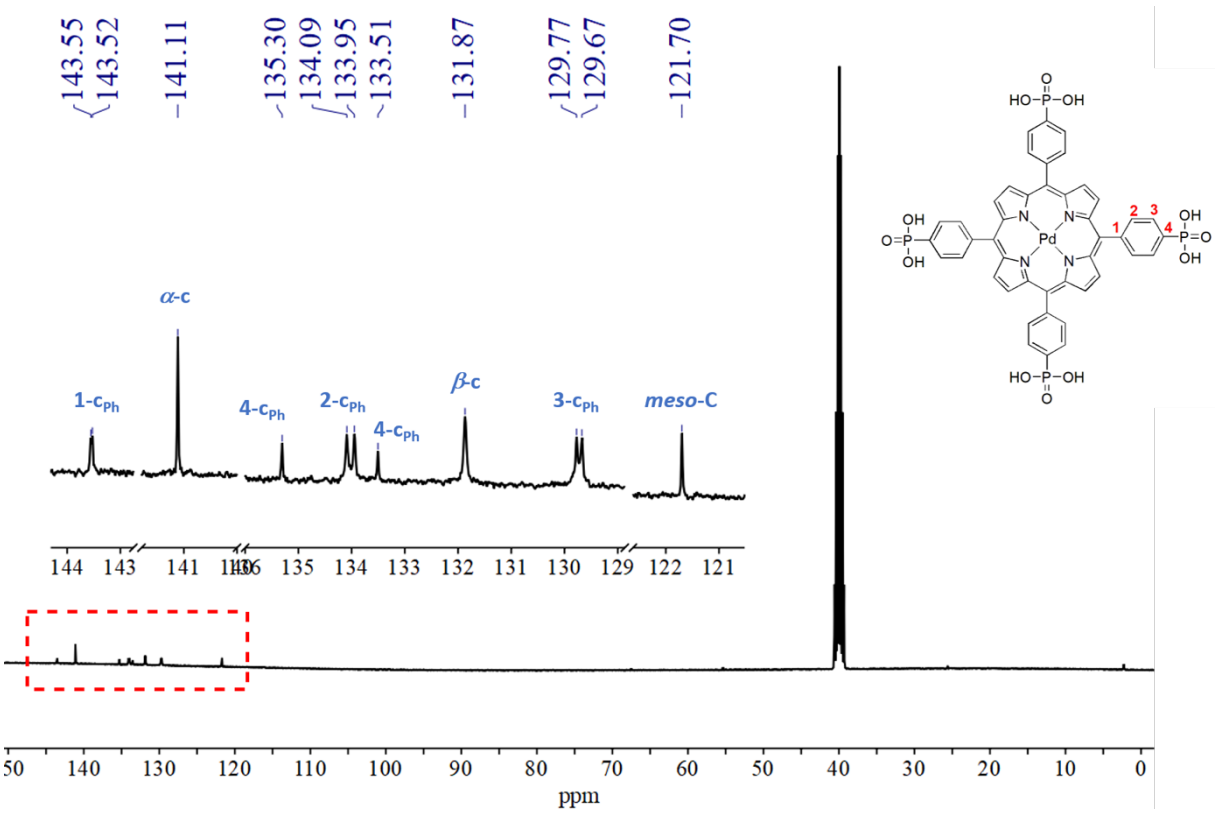

Figure S45. ^{1}H NMR spectrum of H_2(TPPP-A) (300 MHz, $CDCl_3$, 298 K).

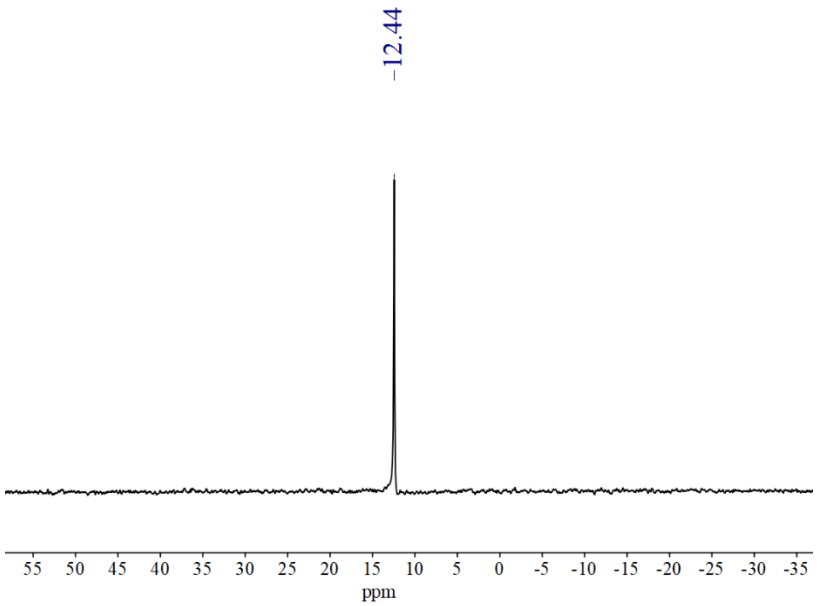

Figure S46. $^{31}P\{^{1}H\}$ NMR spectrum of H_2(TPPP-A) (121 MHz, $CDCl_3$, 298 K).

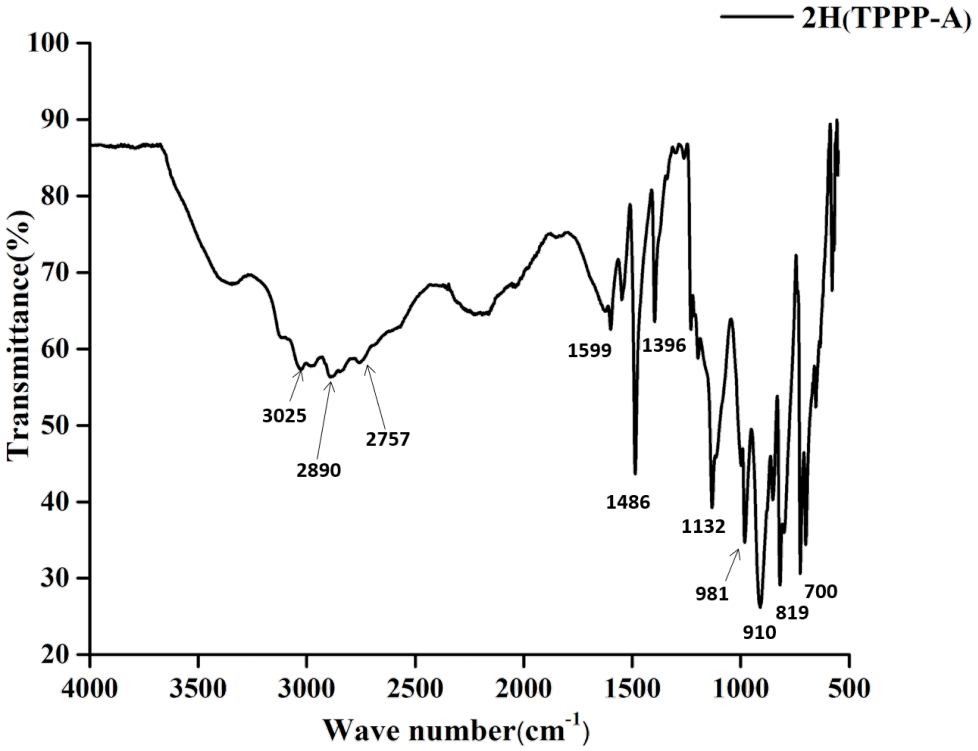

Figure S47. FT-IR spectrum of H_2(TPPP-A) (neat).

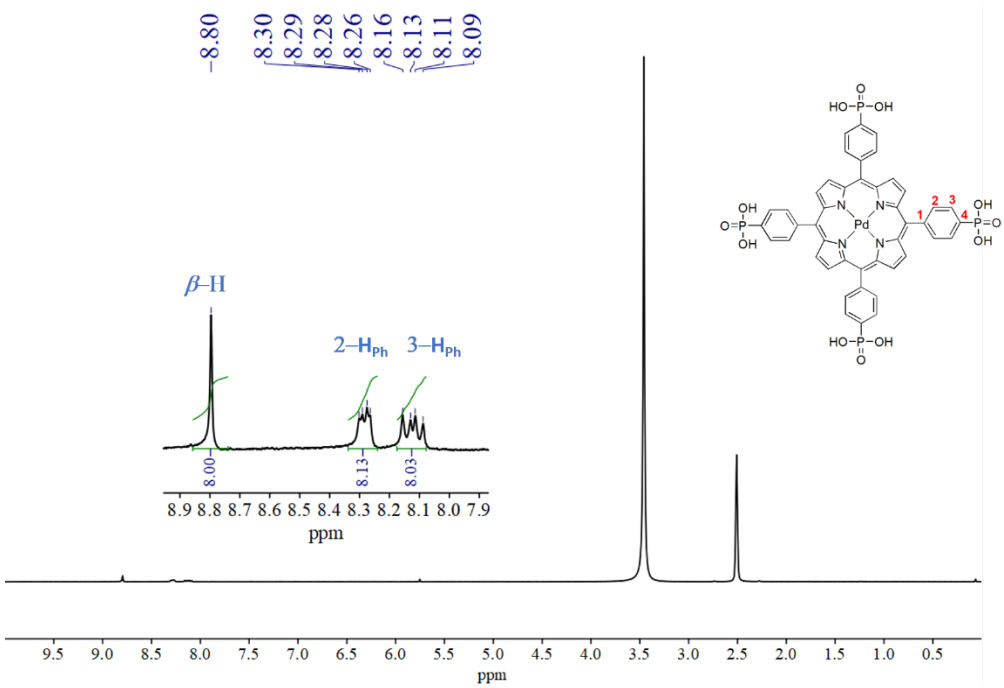

Figure S48. ^{1}H NMR spectrum of Pd(TPPP-A) (300 MHz, $CDCl_3$, 298 K).

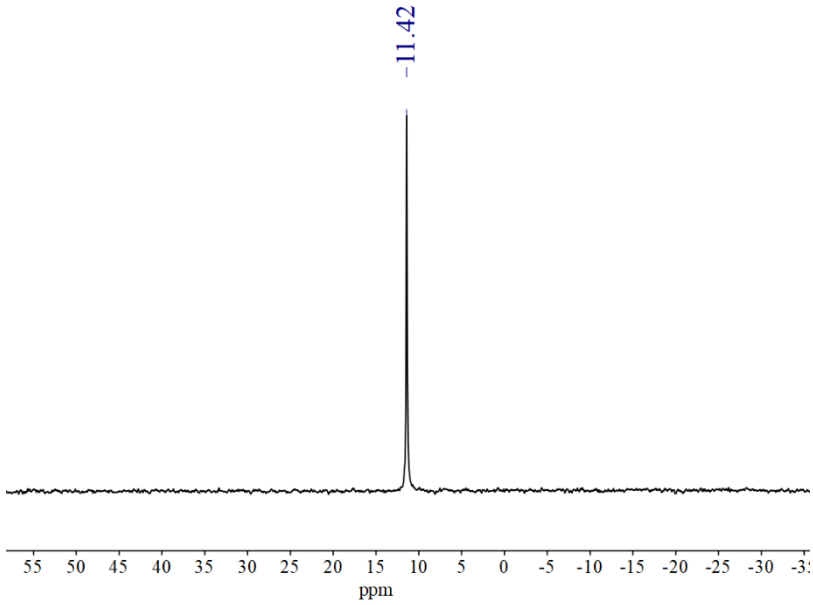

Figure 49. $^{31}P\{^{1}H\}$ NMR spectrum of Pd(TPPP-A) (121 MHz, $CDCl_3$, 298 K).

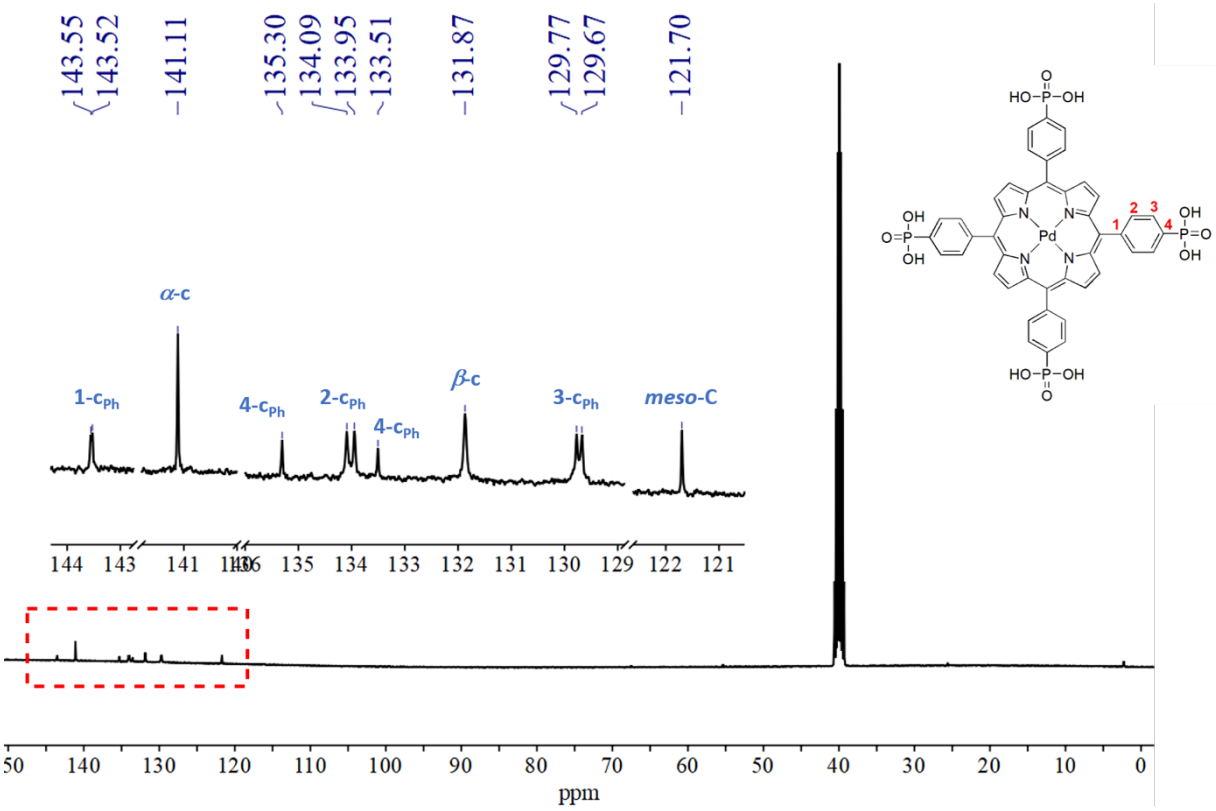

Figure S50. $^{13}C\{^{1}H\}$ NMR spectrum of Pd(TPPP-A) (75 MHz, $CDCl_3$, 298 K).

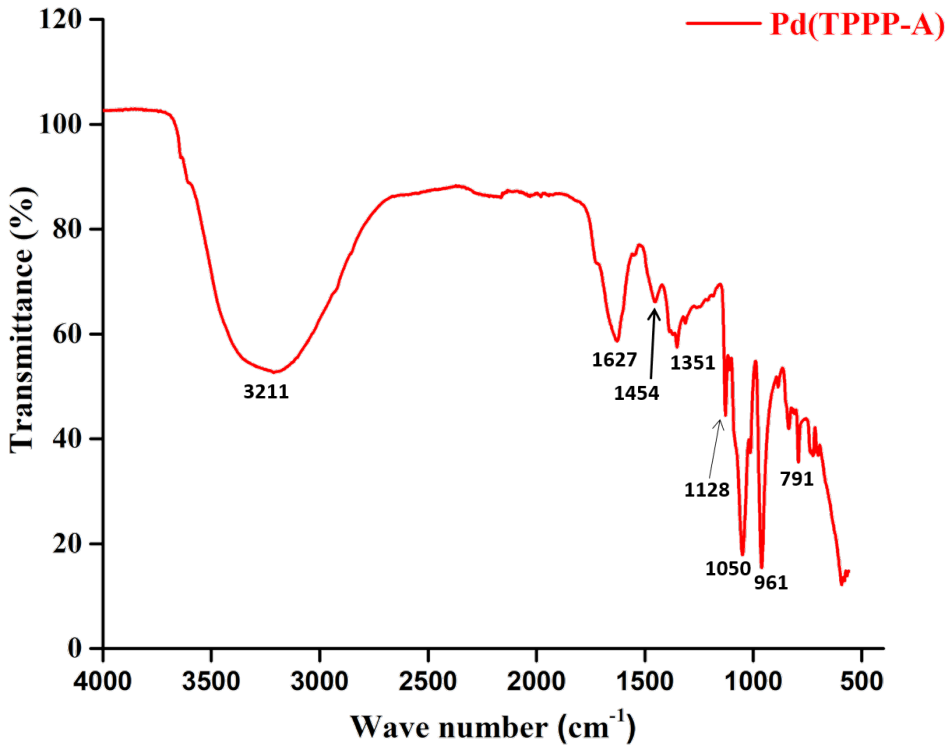

Figure S51. FT-IR spectrum of Pd(TPPP-A) (neat).

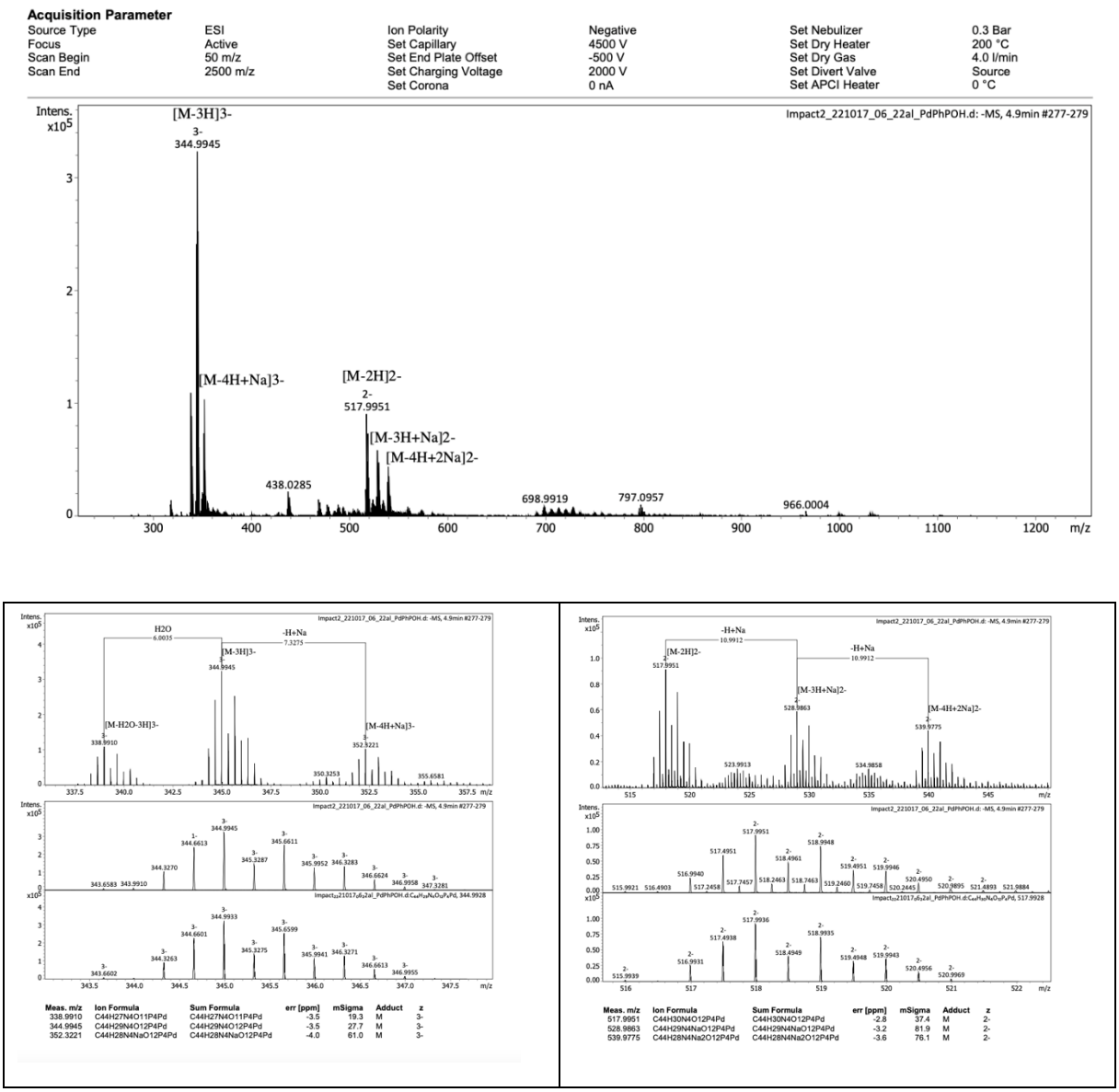

Figure S52. HRMS (ESI) spectrum of Pd(TPPP-A).

10. References

1. P. Kubát, K. Lang and P. Anzenbacher, *Biochim. Biophys. Acta,* 2004, **1670**, 40–48.
2. K. M. Kadish, P. Chen, Y. Y. Enakieva, S. E. Nefedov, Y. G. Gorbunova, A. Y. Tsivadze, A. Bessmertnykh-Lemeune, C. Stern and R. Guilard, *J. Electroanal. Chem.*, 2011, **656**, 61–71.
3. T. Rhauderwiek, K. Wolkersdörfer, S. Øien-Ødegaard, K.-P. Lillerud, M. Wark and N. Stock, *Chem. Commun.*, 2018, **54**, 389–392.
4. M. Maares, M. M. Ayhan, K. B. Yu, A. O. Yazaydin, K. Harmandar, H. Haase, J. Beckmann, Y. Zorlu and G. Yücesan, *Chem. – Eur. J.*, 2019, **25**, 11214–11217.
5. S. K. Hau, Y.-J. Cheng, H.-L. Yip, Y. Zhang, H. Ma and A. K. Y. Jen, *ACS Appl. Mater. Inter.*, 2010, **2**, 1892–1902.
6. D. Deniaud, B. Schollorn, D. Mansuy, J. Rouxel, P. Battioni and B. Bujoli, *Chem. Mater.*, 1995, **7**, 995–1000.
7. D. Deniaud, G. A. Spyroulias, J.-F. Bartoli, P. Battioni, D. Mansuy, C. Pinel, F. Odobel and B. Bujoli, *New J. Chem.*, 1998, **22**, 901–905.
8. J. B. Kim, J. J. Leonard and F. R. Longo, *J. Am. Chem. Soc.*, 1972, **94**, 3986–3992.
9. R. Kumar, P. Yadav, A. Kumar and M. Sankar, *Chem. Lett.*, 2015, **44**, 914–916.
10. J. S. Lindsey, H. C. Hsu and I. C. Schreiman, *Tetrahedron Lett.*, 1986, **27**, 4969–4970.
11. J. S. Lindsey and R. W. Wagner, *J. Org. Chem.*, 1989, **54**, 828–836.
12. SADABS, SADABS, *Bruker AXS, Madison, WI* (after 2013).
13. G. Sheldrick, *Acta Crystallogr., Sect. C: Struct. Chem.*, 2015, **71**, 3–8.
14. G. Sheldrick, *Acta Crystallogr., Sect. A: Found. Adv.,* 2015, **71**, 3–8.
15. P. van der Sluis and A. L. Spek, *Acta Crystallog., Sect. A: Found. Chem.*, 1990, 46, 194-201.
16. A. Spek, *Acta Crystallog., Sect. D: Struct. Biol.*,, 2009, 65, 148-155.